

Naval Research Laboratory

Washington, DC 20375-5000



AD-A239 286



NRL Memorandum Report 6860

## The Predominant Role of Sorbent Phase Swelling or Modulus Changes in Determining the Responses of Polymer-Coated Surface Acoustic Wave Vapor Sensors

JAY W. GRATE, MARK KLUSTY,\* ANDREW MCGILL,\*\*  
MICHAEL H. ABRAHAM,<sup>†</sup> GARY WHITING<sup>†</sup> AND JENIK ANDONIAN-HAFTVAN<sup>†</sup>

*Surface Chemistry Branch  
Chemistry Division Division*

*\*Present address: Microsensor Systems, Inc.  
6800 Versa Center  
Springfield, VA 20744*

*\*\*Geo-Centers, Inc.  
10903 Indian Head Highway  
Fort Washington, MD 20744*

*<sup>†</sup>University College London  
Chemistry Dept.,  
London WC1H 0AJ,  
United Kingdom*

August 10, 1991

91-07434



Approved for public release; distribution unlimited.

91 8 09 02

REPORT DOCUMENTATION PAGE			Form Approved OMB No 0704-0188	
Public reporting burden for this collection of information is estimated to average 1 hour per response, including the time for reviewing instructions, searching existing data sources, gathering and maintaining the data needed, and completing and reviewing the collection of information. Send comments regarding this burden estimate or any other aspect of this collection of information, including suggestions for reducing this burden, to Washington Headquarters Services, Directorate for Information Operations and Reports, 1215 Jefferson Davis Highway, Suite 1204, Arlington, VA 22202-4302, and to the Office of Management and Budget, Paperwork Reduction Project (0704-0188), Washington, DC 20503.				
1. AGENCY USE ONLY (Leave blank)	2. REPORT DATE 1991 August 10	3. REPORT TYPE AND DATES COVERED		
4. TITLE AND SUBTITLE The Predominant Role of Sorbent Phase Swelling or Modulus Changes in Determining the Responses of Polymer-Coated Surface Acoustic Wave Vapor Sensors			5. FUNDING NUMBERS  61-1639-E1	
6. AUTHOR(S) Jay W. Grate, Mark Klusty,* R. Andrew McGill,** Michael H. Abraham, <sup>†</sup> Gary Whiting, <sup>†</sup> and Jenik Andonian-Haftvan <sup>†</sup>				
7. PERFORMING ORGANIZATION NAME(S) AND ADDRESS(ES)  Naval Research Laboratory Washington, DC 20375-5000			8. PERFORMING ORGANIZATION REPORT NUMBER  NRL Memorandum Report 6860	
9. SPONSORING / MONITORING AGENCY NAME(S) AND ADDRESS(ES)  Office of Naval Technology Naval Surface Warfare Center Dahlgren, VA 22448-5000			10. SPONSORING / MONITORING AGENCY REPORT NUMBER	
11. SUPPLEMENTARY NOTES *Present address: Microsensor Systems, Inc., 6800 Versa Center, Springfield, VA 20744 **Geo-Centers, Inc., 10903 Indian Head Highway, Fort Washington, MD 20744, <sup>†</sup> University College London, Chemistry Dept., London WC1H 0AJ, United Kingdom				
12a. DISTRIBUTION / AVAILABILITY STATEMENT  Approved for public release; distribution unlimited.			12b. DISTRIBUTION CODE	
13. ABSTRACT (Maximum 200 words)  The sorption of vapors by fluoropolyol, poly(epichlorohydrin), and poly(isobutylene) is examined by gas-liquid chromatography (GLC) and these results are compared with the responses of surface acoustic wave (SAW) vapor sensors coated with the same polymers. The sensor responses exceed those which can be attributed to gravimetric effects, indicating that the SAW devices are responding to some other change in the coating properties. A model is developed to estimate the effect of polymer swelling on SAW sensor responses. The model is based on the use of partition coefficients determined by GLC as an independent measure of polymer mass loading, and polymer thermal expansion on SAW surfaces as a measure of volume change effects which is independent of mass loading effects. Both experimental comparisons and the model indicate that swelling effects can be ca. 4 times greater than mass-loading effects. The likely mechanism by which swelling influences the SAW sensor response is via reductions in the modulus of the polymer overlayer.				
14. SUBJECT TERMS  Surface acoustic wave, Vapor sensor, Swelling Modulus, Partition coefficient, Gas-liquid chromatography			15. NUMBER OF PAGES 54	
			16. PRICE CODE	
17. SECURITY CLASSIFICATION OF REPORT UNCLASSIFIED	18. SECURITY CLASSIFICATION OF THIS PAGE UNCLASSIFIED	19. SECURITY CLASSIFICATION OF ABSTRACT UNCLASSIFIED	20. LIMITATION OF ABSTRACT UL	

CONTENTS

INTRODUCTION ..... 1

EXPERIMENTAL SECTIONS ..... 5

RESULTS AND DISCUSSION ..... 13

ACKNOWLEDGEMENT ..... 48

REFERENCES ..... 49



A-1

# THE PREDOMINANT ROLE OF SORBENT PHASE SWELLING OR MODULUS CHANGES IN DETERMINING THE RESPONSES OF POLYMER-COATED SURFACE ACOUSTIC WAVE VAPOR SENSORS

## INTRODUCTION

For many years, vapor sensors based on surface acoustic wave (SAW) devices coated with non-conducting, non-volatile, liquids or polymers have been described as gravimetric sensors (1-6). (Reviews of SAW chemical sensors and other piezoelectric sorption detectors can be found in references 5-11.) The role of the liquid or polymer film on the sensor surface is to collect and concentrate vapor molecules from the gas phase by sorption. The SAW device responds to changes in the physical properties of the film as the vapor is sorbed. It is customary to monitor the frequency of the device in an oscillator circuit. The frequency is known to decrease in response to increases in mass on the sensor surface. Because the normal response of a SAW sensor to vapors is also a decrease in frequency, it has generally been assumed that these responses are primarily due to the mass of the vapor which is sorbed.

It is also known that the SAW device should respond to decreases in the modulus of the overlay film with a decrease in frequency (3,12). One might expect that vapor sorption would soften the film. However, this potential contribution to SAW vapor sensor response has been difficult to evaluate because the precise moduli of the overlay films with and without sorbed vapor are not known. Polymer relaxation processes occurring during vapor sorption have also been demonstrated as a mechanism for SAW vapor sensor response (13). For the specific case examined, relaxation at some vapor concentrations caused anomalous responses in a direction opposite to that of a mass-loading response. The observed increases in sensor frequency were attributed to the influence of decreases in the viscosity of the polymer overlayer.

We propose that liquid or polymer phase *swelling* makes a significant contribution to SAW vapor sensor responses, and that the swelling response may exceed the gravimetric response. This swelling response operates in the same direction as the gravimetric response, effectively multiplying the sensitivity of the sensor. In terms of existing models, the probable effect of swelling is to reduce the modulus of the sorbent material. However, we choose to discuss our model in terms of swelling because we can estimate the volume increase of the film on vapor sorption and its effect on sensor frequency, whereas we have no way to estimate the modulus change on vapor sorption.

Our motivation for developing this model arose from our efforts to experimentally confirm the gravimetric nature of SAW vapor sensor responses. Although the mass sensitivity of bare SAW devices is well established, the precise role of mass-loading in the responses of polymer-coated SAW sensors has been less certain. Indeed, the evaluation of gravimetric contributions to SAW vapor sensor responses has faced a problem similar to that faced in evaluating modulus contributions. The actual mass of sorbed vapor is seldom known. It has only been known that vapor is sorbed and that the direction of SAW sensor response is consistent with a gravimetric mechanism.

Our approach has been to use partition coefficients as a method of determining the vapor sorption into materials which are used on SAW sensors (1). The partition coefficient,  $K$ , is simply the ratio of the concentration of vapor in the sorbent phase,  $C_s$ , to the concentration of vapor in the vapor phase,  $C_v$ .

$$K = C_s / C_v \quad (1)$$

If  $K$  and  $C_v$  are known, then the product  $C_v K$  gives the concentration of the vapor in the sorbent phase, and hence its mass. We derived an equation relating SAW vapor sensor responses,  $\Delta f_v$ , to the amount of sorbent phase on the sensor surface expressed as a frequency shift,  $\Delta f_s$ , the density of the sorbent phase,  $\rho_s$ , the concentration of the vapor in the vapor phase, and the partition coefficient (1).

$$\Delta f_v = \Delta f_s C_v K / \rho_s \quad (2)$$

It must be emphasized that eq 2 was derived assuming the sensor's response is entirely due to mass-loading effects. The logical relationship between SAW and quartz crystal microbalance (QCM) vapor sensor responses and partition coefficients had been noted previously (3,14-16). A relationship between partition coefficients and flexural plate wave (FPW) vapor sensors has recently been derived (17).

Eq 2 predicts that a SAW vapor sensor's response should be proportional to the amount of vapor sorbed into the film, which is clearly reasonable, and that the sensor's responses should be related to partition coefficients, assuming that the vapor is absorbed into the bulk of the sorbent phase. This equation also makes a quantitative prediction for SAW vapor sensor responses. If the partition coefficients are independently known, one can calculate the SAW frequency decreases expected due to mass-loading and compare them with observed sensor responses.

We previously reported a study where we used gas-liquid chromatography (GLC) to determine the partition coefficients of many vapors into a material we call fluoropolyol (1). We denote these partition coefficients by  $K_{GLC}$ . The responses of fluoropolyol-coated SAW vapor sensors to several of the same vapors were used to back-calculate apparent partition coefficients, which we denote  $K_{SAW}$ , using eq 2. The  $K_{SAW}$  and  $K_{GLC}$  values were compared. A general correlation between SAW sensor responses and partition coefficients was clearly validated. The ranking of vapors according to the magnitude of the  $K_{SAW}$  values was identical to the ranking determined from  $K_{GLC}$  values. In addition, most of the  $K_{SAW}$  values were of the correct order of magnitude. However, quantitative agreement was only approximate. In cases where the vapors' sorption isotherms (as inferred from the shapes of the SAW sensor calibration curves) were significantly curved concave downward, the  $K_{SAW}$  values were lower than  $K_{GLC}$  values. These results could be logically ascribed to the fact that  $K_{GLC}$  values refer to the vapor at infinite dilution, whereas the  $K_{SAW}$  values were determined from measurements at higher finite vapor concentrations where the relative vapor sorption was actually less. However, if the sorption isotherms were not curved,  $K_{SAW}$  values were greater than  $K_{GLC}$  values.

As we began comparing  $K_{GLC}$  values and  $K_{SAW}$  values for other polymers we were surprised to find that although a proportionality between  $K_{SAW}$  and  $K_{GLC}$  remained valid,  $K_{SAW}$  values continued to be higher than  $K_{GLC}$  values, often significantly so. In an effort to resolve these differences, we re-examined both our SAW and GLC methods. Partition coefficients determined by different individuals at different times on different GLC columns using the same sorbent phases were in agreement. We could find no problems with our GLC method. We also took care to be certain that SAW and GLC measurements were made on samples from the same batch of each polymer. This insured that any differences we observed could not be due to differences in the materials.  $K_{SAW}$  values remained higher than  $K_{GLC}$  values, exactly as before.

We anticipated, however, that we could improve our SAW experiments. Previously, our sensor temperatures were monitored (at ca. 35°C) but not actively controlled, so we began actively controlling our sensor temperatures to 25°C, the same temperature as our GLC experiments. In addition, we upgraded to newer vapor generation equipment in which the bubbler vapor sources were actively thermostatted (18). On our old vapor generation system, bubbler vapor sources had not been thermostatted, and vapor outputs could vary somewhat with laboratory temperatures (19). We meticulously fine-tuned and calibrated our new instrument (18), and our calibrations were in good agreement with concentrations calculated from published vapor pressures and the ideal gas law.

We found that  $K_{SAW}$  values continued to be higher than  $K_{GLC}$  values. In fact, on re-examining fluoropolyol-coated SAW sensors, we found that we obtained somewhat higher  $K_{SAW}$  values than before (as might be expected since our sensor temperatures were now 10°C lower than in the previous study). We then investigated vapor sorption into coatings on SAW devices of various frequencies, and found that SAW frequency was not a significant factor in determining  $K_{SAW}$  values. Regardless of sorbent polymer, SAW device frequency, or vapor generation equipment, it became apparent that  $K_{SAW}$  values calculated according to eq 2 assuming a strictly gravimetric response are consistently higher than  $K_{GLC}$  values when the SAW and GLC measurements are conducted at the same temperature. Our extensive efforts to find and eliminate any sources of systematic error in our measurements confirmed that this result was real. Therefore, mass-loading cannot be the only response mechanism involved when vapor is sorbed into the polymer on a SAW sensor surface.

In this paper, we present experimental results on the sorption of vapors into three polymers at 25°C as determined by GLC, the responses of SAW vapor sensors at 25°C using the same polymers as sorbent phases, and the effects of polymer thermal expansion on polymer-coated SAW sensor frequencies. We then develop a model which represents SAW vapor sensor responses as a sum of gravimetric and swelling effects. The effects (on SAW sensor frequencies) of sorbent phase volume increases due to swelling are estimated from the measured effects of volume increases due to thermal expansion. Our experimental evidence and our model indicate that gravimetric effects account for only a fraction of the actual sensor response.

## EXPERIMENTAL SECTIONS

**Materials.** Fluoropolyol was obtained from Jim Griffith of the NRL Chemistry Division and is the same material used in past chemical sensor investigations (1,2,20,21). It can be synthesized by the methods described by Field (22). The density of fluoropolyol is 1.653 at 25°C and 1.604 at 60°C (1). Poly(isobutylene), low molecular weight, was obtained from Aldrich: average M.W. 380,000, density 0.918, glass transition temperature -76°C. Poly(epichlorohydrin) was obtained from Aldrich: density 1.36.

The liquid organic solvents used to generate vapor streams were commercial chemicals of 99% or greater purity, except nitromethane (Fisher certified ACS, Assay 95.4%). The solutes used in the chromatographic measurements were also commercial materials used as received.

**Gas-Liquid Chromatographic Measurements.** Polymer/gas partition coefficients were determined by GLC using the instrumentation and methodology described in detail in reference 23 and also used in reference 1. The Ostwald solubility coefficient denoted with an L in reference 23 is identical with the partition coefficient denoted in this paper with a K and defined in eq 1. Polymer stationary phases were coated on acid-washed silanized Chromosorb supports (Phase Separations Limited), see Table 1, and packed in glass columns. Partition coefficients are determined from solute retention times as follows: partition coefficients are first determined for a series of standard solutes (normally n-alkanes) using He as the carrier gas and a thermal conductivity detector. The relevant corrections are applied to the retention volumes measured (23). The K values are calculated from the ratio of the adjusted retention volume,  $V_N$ , to the volume of the stationary phase,  $V_L$ :  $K = V_N/V_L$ . Repeated determinations (typically 3 to 5) are made on each standard solute, and standard deviations in log K are typically 0.01 log unit or less. Relative log K values are then determined for many solutes using nitrogen as the carrier gas and flame ionization detection. A standard solute of similar retention to the solute in question is coinjected for each measurement. Relative retention times are converted to absolute K values by using the known absolute K values of the standard solutes as described in reference 23. All chromatographic measurements were conducted at 25°C except for a series of measurements at 60°C on fluoropolyol.

Table I. GLC Column Details.

Polymer:	Fluoropolyol	Poly(isobutylene)	PIB	Poly(epichlorohydrin)	PECH
Abbreviation:	FPOL	PIB	PIB	PECH	PECH
Determination:	A	A	B	A	B
Support:	Chromosorb G.A.W.DMCS	Chromosorb G.A.W.DMCS	Chromosorb W.A.W.DMCS	Chromosorb G.A.W.DMCS	Chromosorb W.A.W.DMCS
Mesh:	60/80	40/60	40/60	40/60	40/60
Loading:	4% <sup>a</sup>	6% <sup>a</sup>	7% <sup>b</sup>	5% <sup>a</sup>	8% <sup>b</sup>

<sup>a</sup> Determined gravimetrically by the mass increase of the support.

<sup>b</sup> Determined gravimetrically by the mass decrease of the support after ashing.

Fluoropolyol, poly(isobutylene), and poly(epichlorohydrin) were first examined in experiments which we label as determinations A. In these cases both short and long columns were prepared for each polymer. To assure that log K values from columns of differing length were the same, a number of solutes in common were studied on the various columns. At a later date, new columns containing poly(isobutylene) and poly(epichlorohydrin) were prepared from scratch on a different support and measurements were made by different individuals in the laboratory. These determinations are labeled B. The poly(isobutylene) and poly(epichlorohydrin) samples used in determinations B are from the same batches of materials used for the SAW experiments. (All fluoropolyol experiments have been conducted using samples from a single batch of this material.)

**Saw Devices and Electronics.** The 158 MHz SAW dual delay line devices and oscillators used in this study were obtained from Microsensor Systems Inc. (Springfield, VA). They were described in detail in reference 1 and are also reported in references 20, 24, and 25. These are dual delay line devices fabricated on ST-cut quartz with aluminum metallization and a thin protective overlayer of silicon dioxide mounted on round 12 pin TO-8 headers with epoxy and gold wirebonds. The oscillator circuitry allows the individual delay line frequencies and their difference frequency to be monitored. Power (5 VDC) was supplied by a Micronta adjustable dual-tracking DC power supply. Devices were covered and sealed with nickel-plated lids, each with two stainless steel tubes for gas flow inlet and outlet. For most experiments, we used these devices as single delay line devices, monitoring the fundamental frequency of an individual delay line and damping out the other delay line with an excess of a soft material. This procedure eliminates cross-talk and increases signal stability (25). We also experimented with devices where we had masked one delay line with a polymer film and etched away the other delay line completely with ammonium bifluoride solution. On dissolving the polymer mask, we were left with a single delay line device, and we monitored the individual delay line frequency as usual. In one case we report the results obtained for a dual delay line sensor with one delay line coated with fluoropolyol and the other delay line bare, monitoring the difference frequency.

The 200 and 400 MHz two port SAW resonators used in this study were obtained from Microsensor Systems, Inc. and were described in detail in reference 26. (The 200 MHz resonator chips are the same as those described in reference 27.) These devices are fabricated on ST-cut quartz with aluminum metallization and a thin protective overlayer of silicon dioxide, one resonator per quartz chip. The devices are mounted on round four pin TO-6 headers with epoxy and gold wirebonds, one device per header. The oscillator circuitry has sockets for two devices, one to be used as a reference and the other as a sampling device. The reference device was covered and sealed with a nickel-plated lid.

The sampling device was covered and sealed with a nickel-plated lid with two stainless steel tubes for gas flow inlet and outlet. Thus the reference is not exposed to test vapors in this configuration. The circuitry allows the individual resonator frequencies and their difference frequency to be monitored. Changes in the frequency of the sampling sensor can be followed from its frequency directly, or from the low frequency difference signal. We monitored the low frequency difference signal during vapor exposure experiments and the individual resonator frequency during polymer thermal expansion experiments.

**Sensor Temperature Control.** The oscillator printed circuit board for the delay line devices was modified so that the socket for the sensor was raised from the PC board by ca. 1.5 cm, using wire-wrap posts as the "stilts". These posts were soldered directly into the position of the original socket on the PC board. Any further separation of the devices from the circuitry resulted in a loss of stable signals. This configuration was mounted vertically in a brass box suspended in a refrigerated circulating water bath with the lid of the sensor pressed against the brass side. Temperatures were monitored with a Cole Parmer Thermister Thermometer (Model N-08502-16) and a YSI 427 small surface probe glued to the bottom outside surface of the header. In this configuration, the probe is bonded to the same piece of metal to which the SAW device is epoxied, but on the opposite side.

*The resonator devices on the Microsensor Systems oscillator boards are separated by 4 cm, center to center. Their temperatures were controlled in our laboratory using a single brass heat sink clamped against the lids of both the reference and sampling devices. Foam insulation was placed around the devices and heat sink. Water from a refrigerated circulating water bath circulated through the brass heat sink. Temperatures were monitored with a Cole Parmer Thermister Thermometer (Model N-08502-16) and a YSI 427 small surface probe glued to the bottom outside surface of the header.*

**Frequency Data Collection.** Frequency measurements were made using Phillips PM6674 frequency counters with TXCO, transferring the data to a microcomputer using the IEEE-488 bus. The resolution varied with the type of experiment being performed, depending on the frequency being monitored and the gate time. Low frequency difference signals from the resonators were monitored during vapor exposure experiments at resolutions typically below 0.1 Hz. Similarly, low frequency difference signals from the dual delay line device during vapor exposure experiments were collected at resolutions typically below 0.1 Hz. Individual delay line frequencies from the 158 MHz dual delay line sensors (operated as a single delay line by damping out the extra delay line - see above) were collected at 2 Hz resolution during vapor testing. Individual resonator or delay line frequencies during thermal expansion experiments were collected at 3 Hz resolution.

**Spray-coated Polymer Films.** Spray-coated films were applied using an airbrush supplied with compressed dry nitrogen and a dilute solution of the polymer in HPLC-grade chloroform (Aldrich). The polymer was applied over the entire surface of the sampling SAW sensor. The individual frequency of the sampling device or delay line was monitored during deposition; the change in frequency provides a measure of the amount of material applied. To begin coating, the airbrush was placed several inches away from the SAW device and spraying was initiated with the nozzle directed away from the device. Then the spray was passed over the device several times, followed by a pause to observe the change in frequency. This process was repeated many times until the desired frequency change was obtained, although with experience one could spray nearly continuously with few pauses. Films causing ca. 250 kHz of frequency change were applied. The absolute film thicknesses decrease with increasing sensor frequency. Thus, 250 kHz films on the 400 MHz devices are only one fourth the average thickness as those on 200 MHz devices, in accord with the rule that mass sensitivity increases with the square of the operating frequency.

Spray-coated films were examined by optical microscopy with a Nikon Optiphot M microscope using reflected light Nomarski differential interference contrast. On clean surfaces the spray coated films appear primarily as small circular domains with raised edges, as if the polymer deposited preferentially at the perimeter of aerosol droplets that landed on the surface. These structures are quite numerous and overlapping. Surface coverage is extensive on the 158 MHz devices and slightly less on the 200 MHz devices. The circular structures are of the same size on the 400 MHz devices, but less numerous.

Surface cleanliness prior to coating influences the wetting and adhesion of the coating material to the sensor surface. Solvent cleaning is adequate for some purposes but we have found that the best results are obtained by cleaning the devices in an rf plasma using a Harrick Plasma Cleaner. We use dry nitrogen as the feed gas, but the plasma is initially an air plasma because we turn on the power as soon as the pressure is low enough to sustain a plasma, with no effort to purge the system first. (Oxygen and air plasmas are more powerful cleaners than nitrogen plasmas because of their oxidizing power.) Typical cleaning time was 15 to 20 minutes.

Sensors with fluoropolyol, poly(epichlorohydrin), and poly(isobutylene) could be prepared with either cleaning method. Some of the vapor exposure data reported in this paper were collected before we began the plasma cleaning method. However all thermal expansion experiments were conducted with films applied to plasma cleaned devices. Good film wetting and adhesion is essential to study these effects. The polymer films were

annealed at 90°C for at least a half hour prior to the experiments, although this made no visible difference in the film morphology.

**Thermal Expansion Experiments.** All polymer thermal expansion experiments were conducted monitoring the individual frequency of the coated sensor. Dry nitrogen at 50 mL/min. (controlled by an electronic mass-flow controller) was routed through a four foot section of 1/8" o.d. 1/16" i.d. Ni tubing coiled in the water bath before being fed into gas inlet tube of the coated sensor. In most experiments, temperatures were ramped between 15 and 45°C at rates between +/-10 and +/-20 °C/hour. A few experiments were conducted over larger temperature ranges (ca. 0 to 90°C). The results were repeatable regardless of the direction or rate of temperature change. At least two determinations were made with each coated sensor. In every case the polymer was then removed from the sensor with solvent and control experiments were carried out to determine the inherent temperature drift of the bare device. Frequency changes due to polymer thermal expansion were determined over the 20 to 30 °C range by subtracting the inherent temperature drift of the device from the observed frequency-temperature profile of the coated device. Results were rounded to the nearest 50 Hz/°C. The temperature drifts of the bare 158 MHz delay lines were typically in the range of 300 to 750 Hz/°C over the 20 to 30°C range. The temperature drifts of the bare 200 MHz resonators averaged ca. 100 Hz/°C over the 20 to 30 °C range, although these profiles (using bare devices) were rather curved, being nearly level around 20°C.

**Isothermal Vapor Exposure Experiments.** All sensors were tested against vapors at 25°C unless otherwise noted. Prior to delivery to the sensor package, vapor streams at room temperature from the vapor generator were passed through nickel tubing coiled in the water bath, or through nickel tubing in a water jacket, or through nickel tubing epoxied to the brass heat sink with heat conductive epoxy.

Vapor streams were generated from bubbler sources and diluted using a Microsensor Systems VG-7000 vapor generation instrument. The bubblers were maintained at 15°C in machined aluminum blocks with inlets and outlets for water from a refrigerated circulating water bath. The carrier gas for bubbler vapors was dry nitrogen supplied to the bubblers at 120 mL/min with electronic flow controllers. The saturated bubbler vapor streams were diluted by the VG-7000 using a pulse-width modulation method with 3 dilution stages. We meticulously fine-tuned this instrument as we describe in detail in reference 18. The experiments in this paper were all conducted with the saturated (at 15°C) vapor streams diluted by a factor of four. This was accomplished by diluting by 50% in each of two consecutive dilution stages. Finally, the instrument output

can be either the diluted vapor stream or clean carrier gas, each at a flow rate of 120 mL/min.

Saturated vapor streams were calibrated gravimetrically by quantitatively trapping the vapor in tared glass tubes containing activated charcoal and molecular sieves in series. A second small charcoal-packed tube was placed in series to check for vapor breakthrough. These calibrations agreed (to within less than +/- 10%) with vapor concentrations calculated from published vapor pressures and the ideal gas law (28). One vapor, toluene, was also calibrated at a one fourth dilution to confirm the correct operation of the dilution mechanism. The saturated concentration determined gravimetrically was 84880 mg/m<sup>3</sup>. The concentration at one fourth dilution, diluting by 50% in each of two dilution stages, averaged 22600 mg/m<sup>3</sup> for three determinations with 20 minute collection times and 21000 mg/m<sup>3</sup> in one determination with a 40 minute collection time. Two calibrations were determined diluting to 25% in one dilution stage and collecting for 40 minutes, both giving values of 21600 mg/m<sup>3</sup>. Clearly, the dilution mechanism operates correctly.

The VG-7000 was connected to a Macintosh computer with a serial communications line. We delivered commands for each experiment using a communications program (Smartcom II); sequences of experiments were programmed using the macro or "autopilot" capabilities of this program.

Sensor exposure experiments were carried out by first generating and equilibrating a vapor stream for 45 min while delivering clean carrier gas to the sensor. Vapor was then delivered to the sensor for 5 min, followed by 10 min of clean carrier gas for sensor recovery, another 5 min of vapor to check response reproducibility, and another 10 min of clean carrier gas. Thus each experiment takes 75 min. Sensor frequency data were collected every 12 sec beginning 10 min prior to the first vapor exposure. The two consecutive exposures were quite reproducible. The numerical data reported in the tables are taken from the frequency shifts observed during the first exposure.

Before each 75 min experiment described above, a 75 min control experiment was run to insure that no residual vapors were present in the instrument that could cause a sensor response. The carrier gas flows and timing of the control experiment were identical to those of the subsequent vapor experiment, except that the bubbler was bypassed. The 45 min equilibration time served to flush out any traces of vapor which may have adsorbed to tubing walls during the previous experiment. Following the sensor frequency during the subsequent 'vapor'/clean carrier gas output cycles provided an experimental determination that the system is adequately flushed. If the sensor frequency shifts were absent or negligibly small, then the response in the subsequent experiment was certain to be due to the vapor from the bubbler selected.

As a further quality check, a 158 MHz dual delay SAW vapor sensor whose response characteristics are well-known to us was always placed in series after the experimental sensor and its responses were monitored. The consistent responses of this sensor from data set to data set confirmed that the programmed vapor streams were being generated and delivered.

**Vapor Exposures while Ramping the Temperature.** These experiments on poly(isobutylene)-coated 158 MHz delay line sensors were conducted in a fashion similar to the thermal expansion experiments with the following changes. Temperatures were ramped over a much larger range, although still at ramp rates between between +/- 10 and +/- 20 °C/hour. The carrier gas flow rate was increased to 120 mL/min. for experiments under dry nitrogen. Experiments exposing the sensor to toluene vapor were conducted generating the toluene vapor from a bubbler maintained in an ice bath at 0°C. This vapor stream was generated at 60 mL/min. Based on published vapor pressures and the ideal gas law, this generates a concentration of 35000 mg/m<sup>3</sup> when the gas is expanded to 25°C. This saturated (at 0°C) toluene vapor stream was diluted with an additional 60 mL/min of carrier gas prior to delivering it to the sensor, yielding a final concentration of 17500 mg/m<sup>3</sup>. Gas and vapor streams were routed through the four foot coil of tubing in the water bath prior to delivery to the sensor as described above. Frequency-temperature curves generated by these experiments are reproducible regardless of the direction of temperature change or the number of prior vapor exposures.

## RESULTS AND DISCUSSION

**Chromatographic Measurements of Partition Coefficients.** Partition coefficients quantifying the sorption of vapor into the polymers we use on SAW sensors were determined by GLC. This is a well established method for making these thermodynamic measurements (29). The accuracy of the GLC instrumentation and methodology we use to determine these coefficients has been evaluated experimentally by comparing GLC partition coefficients and those determined by head space analysis (23). The latter technique is in principle the more straightforward technique because the concentrations of solute in the gas and solvent phases are determined separately by direct analytical methods. Unfortunately it suffers from a lack of precision and the measurements are much more time-consuming than GLC measurements. GLC measurements can be more precise but are potentially affected by secondary effects other than the absorption process of interest. Potential secondary effects that might occur include adsorption of the solute at the support surface, at the polymer/gas interface, or both. In a study by the present authors excellent agreement between GLC and head space measurements was demonstrated for both non-polar and medium polarity stationary phases (23). These results confirm the accuracy of the GLC methodology we use.

The polymer/gas partition coefficients determined for fluoropolyol, poly(isobutylene), and poly(epichlorohydrin) are given in Table II. The vapors listed are those in common with our SAW sensor measurements. Partition coefficients for many more vapors were also determined and these will be used in developing linear solvation energy relationships (LSER) and structure property relationships in future publications. Two columns of partition coefficients are listed for fluoropolyol. The first contains values determined at 25°C. At this temperature some of the retention times were very long and peak profiles were broad. Tailing was sometimes observed. Additional measurements were made at 60°C and these values were used to estimate partition coefficients at 25°C using a temperature correlation we reported previously (1). These estimated values are in the second column of fluoropolyol partition coefficients. The chromatography at 60°C was significantly improved with better peak shapes and shorter retention times. The choice of fluoropolyol  $K_{SAW}$  values (i.e., temperature-correlated to 25°C or those measured directly at 25°C) is not particularly important for the GLC/SAW comparisons being made in this paper, however. One reaches the same conclusions regardless of which values are used. Most of the fluoropolyol/gas partition coefficients published previously were the temperature-correlated values (1). (In one case, butanone, the origin of the published partition coefficient was not correctly identified.)

Table II. Log K<sub>G</sub>L<sub>C</sub> Values for Three Polymers at 25°C

Polymer. Determination:	FPOL	FPOL <sup>a</sup>	PIB	PIB	PECH	PECH
	A	A	A	B	A	B
isooctane	1.22	1.22	2.24	2.28	1.72	
1,2-dichloroethane	1.85	1.94	2.07		2.82	2.74
toluene	2.37	2.64	2.74	2.76	3.08	3.03
nitromethane	2.85	2.85	1.60	1.55	2.38	2.89
butanone	3.66	3.48	1.84	1.80	2.73	2.61
2-propanol						2.17
1-butanol	3.84	3.66	2.33	2.20	3.23	3.02

<sup>a</sup> These are estimated values from data collected at 60°C and a correlation between data at 25 and 60°C. See reference 1. All other data in the table were collected at 25°C as described in the Experimental Section.

Two columns of partition coefficients are listed for each of the other two polymers and these columns are labeled A and B. Retention times for vapors on these polymers were much more easily measured and all values were determined at 25°C. Nevertheless, we repeated measurements on each polymer as described in the Experimental Section, for the reasons stated in the Introduction. There were a total of twenty-four solutes in common between determinations A and B for poly(epichlorohydrin). Agreement between the sets was very good except for two outliers, one of which is in Table II (nitromethane). Removing these two we obtained the following correlation for the remaining twenty-two solutes.

$$\begin{array}{l} \text{PECH:} \quad \log K_{(A)} = 1.02 (+/-0.03) \log K_{(B)} + 0.05 (+/-0.08) \quad (3) \\ \quad \quad \quad n = 22 \quad \quad r = 0.993 \quad \quad SD = 0.09 \end{array}$$

There were nineteen solutes in common between the GLC data sets for poly(isobutylene), two of which were outliers. Removing these two we obtained the following correlation for the remaining seventeen solutes.

$$\begin{array}{l} \text{PIB:} \quad \log K_{(A)} = 1.07 (+/-0.04) \log K_{(B)} + 0.10 (+/-0.08) \quad (4) \\ \quad \quad \quad n = 17 \quad \quad r = 0.991 \quad \quad SD = 0.07 \end{array}$$

In determination B the  $K_{\text{GLC}}$  values of alcohols on poly(isobutylene) were systematically lower than those from determination A by about .2 log units, possibly due to a support interaction in determination A. Polar hydrogen-bond donating alcohols are particularly prone to this type of interaction when the stationary phase has low polarity. Removing the alcohols, we obtained the following correlation for the remaining fourteen solutes.

$$\begin{array}{l} \text{PIB:} \quad \log K_{(A)} = 1.00 (+/-0.02) \log K_{(B)} + 0.01 (+/-0.05) \quad (5) \\ \quad \quad \quad n = 14 \quad \quad r = 0.997 \quad \quad SD = 0.04 \end{array}$$

In general, eliminating a few outliers, the agreement between determinations A and B on both polymers is 0.1 log units or less.

The most likely source of systematic error in the GLC partition coefficients is in the measurement of the amount of stationary phase in the column. The A and B determinations for poly(isobutylene) and poly(epichlorohydrin) measured the stationary phase loading by

different methods. In the first cases, loading was measured by the mass increase of the support. In the second case the loading was measured by the mass decrease of the column after ashing. The agreement between the partition coefficients determined by these two methods provides further confidence that our values are repeatable and accurate.

Of the three polymers investigated in this study, fluoropolyol was the most troublesome because of its extremely "polar" character and the long retention times of vapors on fluoropolyol-coated columns. In retrospect, it was a difficult phase for our first investigations (1).

**Measurements of Polymer-coated SAW Sensor Responses.** The responses of polymer-coated SAW sensors to a variety of organic vapors were determined as described in the Experimental Section. The test vapors and their concentrations are given in Table III. These vapors include non-polar, dipolar, polarizable, hydrogen-bond basic, and hydrogen-bond acidic species. The SAW devices used include 158 MHz delay line devices, 200 MHz resonator devices, and 400 MHz resonator devices. In a previous study, the mass per unit area sensitivities of all these devices were experimentally calibrated (26). The experimental results were in excellent agreement with theoretical predictions, including the prediction that mass per unit area sensitivities increase with the square of the SAW device frequency. In addition, this study demonstrated that polymer coatings could be applied by either the Langmuir-Blodgett method or by the spray coating method, and the resulting differences in polymer morphology did not affect the steady-state response levels in tests against vapor challenges.

The temperatures of all the sensors (with one exception) were controlled by placing them in contact with thermostatted heat sinks, and temperatures were monitored with surface-reading thermistors bonded directly to the header on which the SAW devices are mounted. The sensors responded to the test vapors with decreases in frequency exactly as one would expect based on mass-loading or decreases in modulus. (Note that individual device frequencies decrease; low frequency difference signals between coated and uncoated sensors increase.) Typical frequency shifts were between 2 and 10 kHz, although this varies with the sorbent coating and the vapor. Noise levels vary with the particular type of SAW device as described in detail previously, with typical noise levels in the range of 2 to 25 Hz (26). Our sensor responses greatly exceeded the noise levels. Sensors responded to vapors rapidly, usually to >90% of the steady-state response within one or two data points after introduction of the vapor, and recovered with equal speed. (Data points were collected every twelve seconds.) A single notable exception involved

**Table III. Vapors, Liquid Densities, and Test Concentrations for SAW Sensor Response Measurements**

Vapor	Concn, mg/m <sup>3</sup>	Liquid Density g/L
isooctane	44980	692
1,2-dichloroethane	65080	1256
toluene	21220	867
nitromethane	16450	1127
2-propanol	17520	805
butanone	53380	785
1-butanol	3768	810

fluoropolyol and isooctane. In these experiments the sensor responses were always quite slow. For this reason we suspect that the observed slow changes are not entirely due to solution processes (which are fast in all other cases), and we do not include isooctane data for fluoropolyol-coated sensors in our tables. The GLC partition coefficients indicate that this vapor is very weakly absorbed by fluoropolyol.

In this paper, we convert the observed SAW sensor responses in Hz to apparent  $K_{SAW}$  values using eq 2 and report the results as logs in the tables. Although we no longer believe that  $K_{SAW}$  values calculated by this method correspond to actual partition coefficients, this method is chosen to facilitate comparisons with  $K_{GLC}$  values. The amounts of sorbent coating on the sensors, in kHz, are reported in the column headings in the tables. The original observed sensor responses in Hz can be easily calculated from the tabulated log  $K_{SAW}$  values, the coating thicknesses in kHz, the coating densities in the Experimental Section, and the test concentrations in Table III, provided that attention is paid to the choice of units (see reference 1). In addition, the original sensor responses in Hz for a few representative sensors will be given in one of the last tables in this paper when evaluating our model for swelling effects.

We have accumulated several data sets of fluoropolyol-coated sensor responses. These results are given in Table IV. Although there is some variation among the less polar vapors, the consistency of the log  $K_{SAW}$  values for the sorption of polar vapors into this polar phase is very good for all sensors at 25°C. (The sensor tested at room temperature is also in good agreement with those thermostatted at 25°C.) Moreover, this consistency is maintained regardless of SAW device frequency, indicating that the responses are primarily due to absorption. Compare, for example, SAW sensors at 200 and 400 MHz. The 400 MHz device has four times the mass per unit area sensitivity of the 200 MHz device. When both are coated with polymer until 250 kHz of frequency shift is observed, the 400 MHz device has one-fourth the mass per unit area of coating and one fourth the volume per unit area of coating. Since absorption depends on the volume of the coating, the 400 MHz device will sorb one fourth the amount of vapor per unit area during vapor exposures, but is four times more sensitive to that mass. As a result, both devices give the same signal in Hz, and the same  $K_{SAW}$  values are calculated (see eq 2). On the other hand, if surface adsorption were the main mechanism, the volume of coating would be irrelevant and the mass per unit area sensitivities dictate that the 400 MHz should give four times the response of the 200 MHz sensor. This clearly was not observed. In general, the thinner the coating and the greater that mass per unit area sensitivity, the greater the role that interfacial adsorption effects should play if they are significant. One can discern a small systematic increase in response on the 400 MHz sensor relative to the 200 MHz sensors, suggesting

that interfacial adsorption contributions to sensor response are beginning to manifest themselves, but the increase is quite small relative to the 400% increase that would be expected if adsorption effects predominated. This effect has been previously been noted for resonator sensors coated with poly(vinyl tetradecanal) (26). Our arguments are expressed in terms of mass-loading effects, but the same result would be derived if the observed responses are due to modulus decreases. Modulus effects also depend on the square of the device operating frequency (3), and modulus is a bulk property of the polymer material.

In the last column of Table IV, we list  $\log K_{SAW}$  values for a fluoropolyol-coated sensor tested at 40°C. In general, vapor sorption and hence sensor responses decrease with temperature, and this is observed. These values determined at 40°C are entirely consistent with our previous report where fluoropolyol-coated 158 MHz SAW sensor temperatures were reported to be 35 +/- 2°C (1). In the latter case, the temperatures were measured with a thermistor placed in the air near the sensors in the oscillator electronics box. We now know that the oscillator electronics generate significant heat, and that sensor temperatures cannot be accurately determined unless the thermistor is placed directly on the sensor package. It is likely that the actual sensor temperatures in the previous study were higher than 35°C.

The  $\log K_{SAW}$  values we have determined from poly(epichlorohydrin)-coated sensors are listed in Table V. Agreement among the three sensors listed is good except for an anomalously large value for isooctane on the 158 MHz delay line. Some variation is observed among the alcohols from device to device with the largest values being obtained on the plasma-cleaned device. This result suggests that an interfacial adsorption effect may make an observable contribution to these responses, since alcohols are expected to hydrogen-bond to the glass surfaces. The agreement between all non-hydrogen bond acid vapors on the 200 MHz devices is quite good.

In Table VI are listed the  $\log K_{SAW}$  values we have determined from the responses poly(isobutylene)-coated 200 MHz SAW resonators. Again, the agreement is very good except the alcohols, which gave larger responses on the plasma-cleaned device. Since this polymer is essentially non-polar, this is the case where we would most expect to see interfacial adsorption effects to manifest themselves with polar vapors. In fact, the differences between the solvent-cleaned and plasma-cleaned sensor responses to alcohols are greatest when the polymer is poly(isobutylene), slightly smaller with poly(epichlorohydrin), and no differences are observed when the polymer is fluoropolyol.

Table IV. Log K<sub>SAW</sub> Values Determined from the Responses of Fluoropolyol-Coated SAW Sensors of Various Types and Frequencies

Polymer:	FPOL 158 Del. <sup>a</sup> Solvent 282 25°C	FPOL 158 Del. <sup>b</sup> Solvent 250 r.t. <sup>e</sup>	FPOL 200 Res. <sup>c</sup> Solvent 258 25°C	FPOL 200 Res. Solvent 247 25°C	FPOL 200 Res. Plasma 251 25°C	FPOL 400 Res. Solvent 312 25°C	FPOL 200 Res. Solvent 247 40°C
1,2-dichloroethane	2.79	2.70	2.82	2.73	2.68	2.97	2.43
toluene	3.36	3.23	3.44	3.35	3.27	3.57	2.92
nitromethane	3.40	3.36	3.41	3.40	3.36	3.47	3.06
butanone	3.67	3.62	3.71	3.71	3.67	3.75	3.42
2-propanol	3.60	3.57	3.68	3.65	3.66	3.71	3.17
1-butanol	4.23	4.20	4.30	4.27	4.28	4.34	3.79

<sup>a</sup> Delay line device operated as a single delay line as described in the Experimental Section.

<sup>b</sup> Dual delay line with one bare side and one coated side, monitoring the difference frequency.

<sup>c</sup> Resonator device.

<sup>d</sup> The frequency decreases by this amount when the coating is applied to the device.

<sup>e</sup> Room temperature. This device is not thermostatted, but unlike the experiments in reference 1, it is not in an enclosed box with other heat-generating electronic components such as a power supply and the oscillator circuits of other sensors.

Table V. Log  $K_{SAW}$  Values Determined from the Responses of Poly(epichlorohydrin)-Coated SAW Sensors

Polymer:	PECH	PECH	PECH
Frequency, MHz:	158	200	200
Device type:	Del. <sup>a</sup>	Res. <sup>b</sup>	Res.
Cleaned by:	Solvent	Solvent	Plasma
kHz of polymer <sup>c</sup> :	237	252	254
Temperature:	25°C	25°C	25°C
isooctane	2.54	2.39	2.37
1,2-dichloroethane	3.23	3.22	3.21
toluene	3.58	3.53	3.54
nitromethane	3.51	3.45	3.47
butanone	3.23	3.22	3.25
2-propanol	2.82	2.78	2.95
1-butanol	3.57	3.52	3.67

<sup>a</sup> Delay line device operated as a single delay line as described in the Experimental Section.

<sup>b</sup> Resonator device.

<sup>c</sup> The frequency decreases by this amount when the coating is applied to the device.

Table VI. Log K<sub>SAW</sub> Values Determined from the Responses of Poly(isobutylene)-Coated SAW Sensors

Polymer:	PIB	PIB
Frequency, MHz:	200	200
Device type:	Res. <sup>a</sup>	Res.
Cleaned by:	Solvent	Plasma
kHz of polymer <sup>b</sup> :	248	280
Temperature:	25°C	25°C
isooctane	3.10	3.12
1,2-dichloroethane	2.71	2.72
toluene	3.41	3.44
nitromethane	2.25	2.25
butanone	2.55	2.59
2-propanol	2.31	2.53
1-butanol	3.06	3.27

<sup>a</sup> Resonator device.

<sup>b</sup> The frequency decreases by this amount when the coating is applied to the device.

We also have data for the responses of a poly(isobutylene) 200 MHz resonator to selected organic vapors (to which it is particularly sensitive) at four temperatures. These were determined by the usual method of discrete vapor exposures under isothermal conditions. Numerical results are reported in Table VII, and the results for two of the vapors are presented graphically in Figure 1, plotting sensor response on a logarithmic scale. (The third vapor, toluene, is omitted only because the data overlap those for isooctane and would complicate the graph.) The linearity of these plots demonstrates that responses are exponentially temperature dependent, at least over the temperature range investigated. This result is consistent with the fact that the sorption of organic vapors varies exponentially with temperature under most conditions.

A novel method of investigating and illustrating the effect of temperature on polymer-coated SAW devices and their responses to vapors is shown in Figure 2. Changes in sensor frequencies are plotted as a function of temperature over a wide temperature range. The top plain line illustrates the effect of temperature on the frequency of a bare device. The bold line was determined using the same device with a film of poly(isobutylene), conducting the experiment under dry nitrogen. The lowest curve was measured with the sensor under a gas stream containing toluene vapor as described in the Experimental. At any single temperature, the difference between the bold line and the lowest curve represents the response of the sensor to the test toluene concentration. The profound effect of temperature on sensor response is dramatically shown by the shape of the curve measured during toluene exposure.

The difference in slopes between the upper two lines illustrates the effect of polymer thermal expansion on sensor frequencies. Sensor frequencies decrease as the temperature rises and the polymer expands. The effect of polymer expansion on sensor frequencies is surprisingly large. We shall expand on this topic below when developing our model for swelling effects .

Measurements of polymer-coated sensor frequencies over large temperature ranges also have the potential to reveal the occurrence of polymer relaxation processes in response to the dynamic motions induced by the high frequency surface waves. If such processes occur and influence sensor frequencies, then they could be relevant to the mechanisms of the sensors' responses to vapors; vapor sorption could also induce such relaxation processes by plasticizing the polymer material. However, the frequency-temperature profile of the poly(isobutylene)-coated device under nitrogen is essentially linear over a large temperature range, and the frequency is decreasing. Poly(epichlorohydrin)- and fluoropolyol-coated devices behave similarly. Therefore we see no indication that any relaxation processes are playing a significant role in our sensors' frequency responses.

Table VII. Responses of a Poly(isobutylene)-coated 200 MHz SAW Resonator<sup>a</sup> to Vapors at Various Sensor Temperatures

	25°C	35°C	45°C	55°C
	Responses in Hz			
isooctane	17898	10839	6802	4548
1,2-dichloroethane	10324	6765	4606	3383
toluene	17774	10064	6503	4383
	Responses as Log K <sub>SAW</sub> <sup>b</sup>			
isooctane	3.12	2.90	2.70	2.52
1,2-dichloroethane	2.72	2.53	2.37	2.23
toluene	3.44	3.19	3.00	2.83

<sup>a</sup> Sensor with 280 kHz of poly(isobutylene).

<sup>b</sup> These values are not corrected for changes in polymer density with temperature.

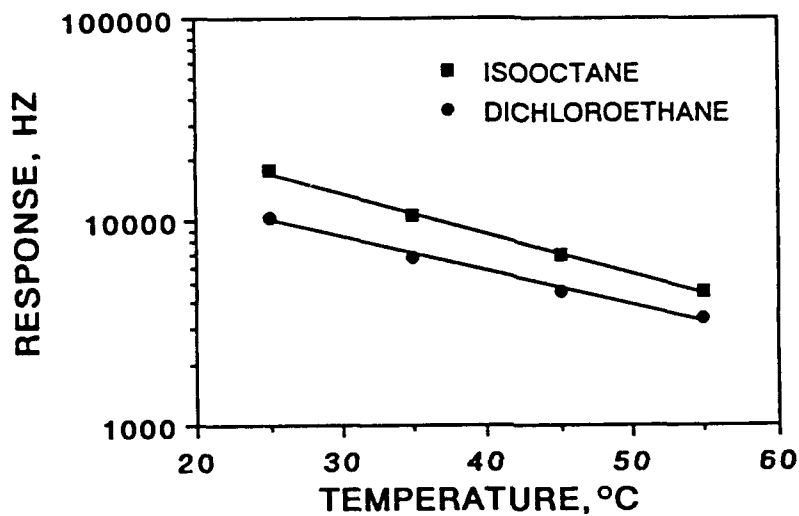


Figure 1. The temperature dependence of the responses of a poly(isobutylene)-coated 200 MHz resonator to isooctane and 1,2-dichloroethane. The responses are plotted on a logarithmic scale. The linearity of each plot demonstrates that sensor response is exponentially temperature dependent. Data for toluene are also linear, but are not shown on this plot because they overlap the isooctane data.

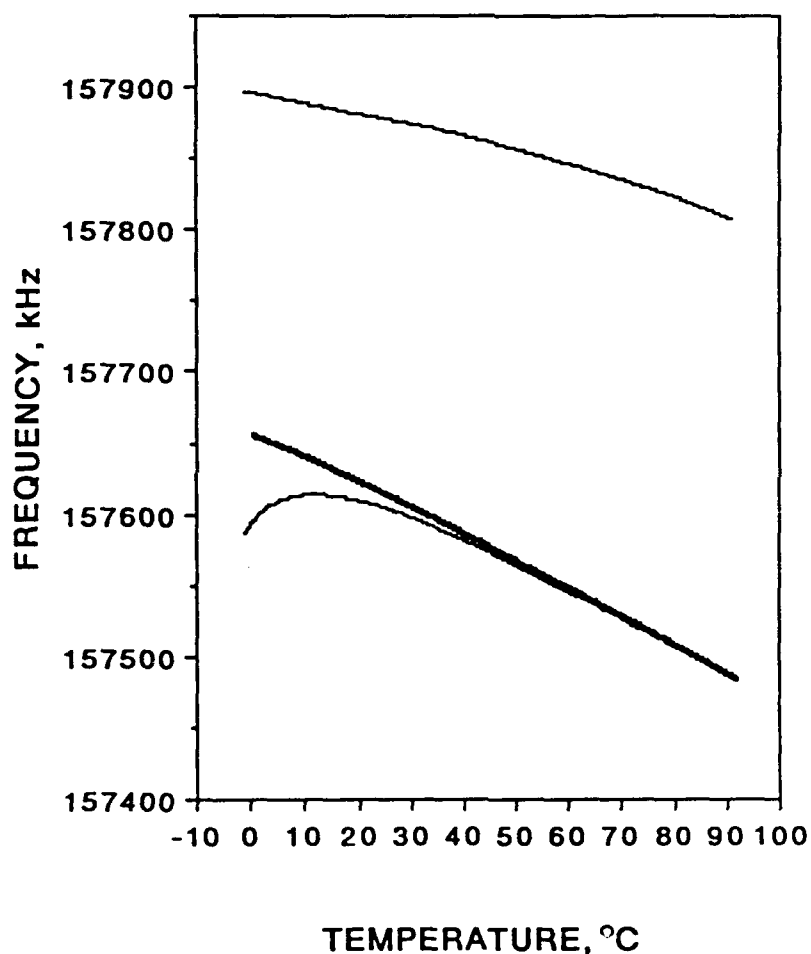


Figure 2. The frequency as a function of temperature of a bare 158 MHz single delay line SAW device (upper plain line), the same device with a 269 kHz poly(isobutylene) coating under dry nitrogen (central bold line), and the poly(isobutylene)-coated sensor under a stream of toluene vapor (lower plain curve). The difference in the slopes of the upper and central line illustrate the effect of polymer thermal expansion on sensor frequency. The difference between the two lines at 25°C gives the thickness of the coating in kHz. The difference between the lower curve and the central line at any temperature gives the response of the sensor to toluene, and the curvature of the lower curve illustrates the exponential dependence of response on temperature.

Polymer thermal expansion is clearly the dominant effect. (It follows that relaxation processes in the homogeneous amorphous polymers we use either do not significantly influence sensor frequency or that they are not occurring in our temperature range at the sensor frequency. This question might be resolved by measuring signal attenuation as well as frequency, but our SAW oscillator circuits are not well suited for such measurements.) Martin and Frye have reported that relaxation processes in a styrene-butadiene-styrene triblock copolymer cause SAW oscillator frequencies to increase in response to increasing temperature or the plasticizing effect of vapors (13). We do not see such frequency increases in our experiments.

**Comparisons of Log  $K_{SAW}$  vs. Log  $K_{GLC}$  Values.** It is evident from the data in the tables that  $K_{SAW}$  values calculated according to eq 2 from the responses of sensors at 25°C are significantly greater than actual  $K_{GLC}$  values. In Figure 3, we have plotted log  $K_{SAW}$  vs. log  $K_{GLC}$  values for the three polymers under investigation. With poly(isobutylene) and poly(epichlorohydrin) the correlation is linear, but the data are above the line representing quantitative agreement. With fluoropolyol the data also fall above the correlation line. However basic vapors, especially butanone, are not as high above the line as the others. Fluoropolyol is a strong hydrogen-bond acid which has specific interactions with bases, and butanone is sorbed in greater quantities than any other vapor. The significance of this will be discussed further below.

In general, log  $K_{SAW}$  values are ca. 0.6 to 0.8 log units higher than log  $K_{GLC}$  values, indicating that calculated  $K_{SAW}$  values are ca. 4 to 6 times greater than they should be if the sensor responses are strictly gravimetric. In other words, if we use eq 2 to predict gravimetric SAW sensor responses, taking  $K_{GLC}$  values as an accurate and independent measure of the mass loading of the sorbent phase, we find that actual SAW sensor responses are significantly greater. We will refer to the difference between gravimetric and actual SAW vapor sensor responses as the "excess" response.

These results are significant result for the interpretation of SAW vapor sensor responses. They indicate that some mechanism in addition to mass-loading is influencing sensor responses. We failed to discern this important difference between SAW and GLC results in our previous report on fluoropolyol-coated sensors for two main reasons (1). First, the choice of fluoropolyol as our first test case complicated matters because so many basic vapors have curved isotherms in this strongly hydrogen-bonding material. Second, the lack of rigorous sensor temperature control resulted in the measurement of  $K_{SAW}$  values at ca. 35°C (or possibly higher) which were lower than they would have been if they had been measured at 25°C.

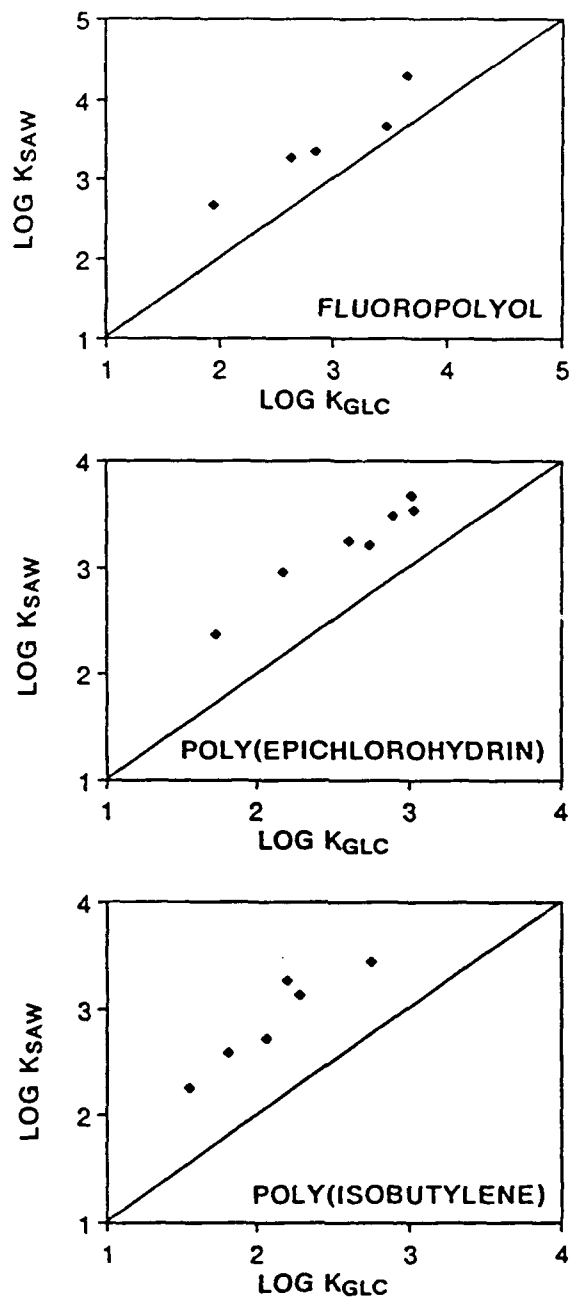


Figure 3. Comparisons of  $\log K_{SAW}$  values and  $\log K_{GLC}$  values, where the  $\log K_{SAW}$  values are calculated from the observed responses of SAW vapor sensors using eq 2 (which assumes responses are strictly gravimetric). The diagonal line in each plot represents one-to-one correspondence. The vapors in the fluoropolyol plot in order of increasing partition coefficients are 1,2-dichloroethane, toluene, nitromethane, 2-butanone, and 1-butanol. On the poly(epichlorohydrin) plot the vapors in order of increasing partition coefficients are isooctane, 2-propanol, 2-butanone, 1,2-dichloroethane, nitromethane, toluene, and 1-butanol. On the poly(isobutylene) plot the vapors in order of increasing partition coefficients are nitromethane, 2-butanone, 1,2-dichloroethane, 1-butanol, isooctane, and toluene.

**A Model for Polymer Swelling Effects.** In an effort to rationalize the magnitudes of the observed SAW sensor responses, we considered the possibility that sorbent phase swelling might contribute to the sensors' responses. After considering a number of analogies that motivate the idea that polymer volume changes should affect SAW frequencies, we will develop a model for swelling effects using experimentally measurable quantities or straightforward estimates derived from experimentally measurable quantities. In this model we do not make any assumptions about the mechanism whereby volume expansion influences surface wave velocities and hence oscillator frequencies. In our treatment of swelling effects, we will consider the sorbent phase to be a polymer above its static glass transition temperature,  $T_g$ . We customarily choose polymers above  $T_g$  for sensor coatings because vapor diffusion in polymers below  $T_g$  can be quite slow.

We begin our model with the observation that the sorption of vapor molecules increases the free volume in the polymer (30). We further note that polymer free volume increases during thermal expansion at temperatures above the  $T_g$  (31). (Below  $T_g$  free volume is relatively constant with temperature.) On this basis we can draw an analogy between volume increases due to vapor sorption and volume increases due to polymer thermal expansion. The proportionality between free volume increases due to vapor sorption and free volume increases due to temperature increases has been discussed by Rogers, assuming that the interactions between the vapor and the polymer are ideal (30). It is also relevant that polymer thermal expansion has a significant effect on SAW frequencies. This effect is evident in the upper lines of Figure 2, where the rate of frequency change is greater for the polymer-coated device than the bare device. The direction of frequency change as the polymer expands is in the same direction as the change caused by increasing the mass per unit area on the SAW surface. It follows logically that volume changes due to swelling might also have significant effects on SAW frequencies, and that the effect should increase SAW vapor sensor responses. Moreover, we realized that polymer thermal expansion provides an experimental method to measure the effects of polymer volume increases on SAW frequencies that is independent of any mass per unit area changes.

We can further motivate our model by noting the results of conventional ultrasonic studies on polymers (32-36). Acoustic velocities decrease as polymer temperatures rise. Concurrently the polymer free volume is increasing, the density is decreasing, and the modulus, which is strongly dependent on density, is decreasing. If the acoustic velocity is measured over a temperature range that includes the polymer  $T_g$ , a discontinuity in the slope of the velocity-temperature plot can be observed. This change in slope correlates with the change in polymer thermal expansion rates at  $T_g$ , leaving little doubt that acoustic

velocities are sensitive to polymer volume changes. (Note that the transition in polymer thermal expansion at  $T_g$  is independent of the probing sonic frequency.)

Similar results have been seen when monitoring the frequencies of polymer-coated flexural plate wave devices as the temperature is raised (17). The slopes of the frequency-temperature plots become steeper at the polymer  $T_g$ . (Note that acoustic velocities and frequencies are directly related.) These results demonstrate that the characteristics observed in conventional ultrasonic studies are also applicable to thin polymer overlayers on planar acoustic devices.

The rate of frequency change associated with the thermal expansion of a polymer layer on a SAW device is quite large. Ballantine and Wohltjen have reported rates attributable to the polymer overlayers on 158 MHz SAW devices of ca. -2 to -4 ppm/°C in experiments in the 40 to 110°C temperature range (37). Their results correspond to -0.3 to -0.6 kHz/°C. We have examined the frequencies of polymer-coated 158 MHz SAW sensors and 200 MHz SAW delay lines over temperature ranges near our sensor operating temperatures. The results are reported in Table VIII. In each case the inherent temperature drift of the bare device has been subtracted from the observed slope of the frequency-temperature plot of the coated device. In the range of 20 to 30°C fluoropolyol induces a temperature drift rate of -0.6 kHz/°C, in agreement with the results of Ballantine and Wohltjen at higher temperatures. Similarly, the rate associated with a film of poly(epichlorohydrin) is -0.7 kHz/°C, and the rate associated with a film of poly(isobutylene) is -1 kHz/°C. The "thicknesses" of the polymer layers on these sensors expressed as frequency shifts were between 240 and 300 kHz.

Typical coefficients of thermal expansion for polymers above their static glass transition temperatures are around 0.0005 or 0.0006 °C<sup>-1</sup> (38,39). Those of our test polymers are given in Table IX and they are in accord with this generalization. Liquid coefficients of thermal expansion are slightly higher with values around 0.001 °C<sup>-1</sup> (40). If we conservatively estimate the SAW frequency response due to polymer thermal expansion as -0.5 kHz/°C and take 0.0005 °C<sup>-1</sup>, or 0.05% per degree, as the coefficient of polymer thermal expansion, we calculate that an expansion of only 0.1% could produce a -1 kHz frequency change. To expand the polymer by 1%, the temperature would have to rise by 20°C, and this could produce a -10 kHz change in SAW sensor signal. This analysis demonstrates quite clearly that small sorbent phase volume increases can have a significant influence on surface wave velocities, and could be quite a significant influence on vapor sensor responses.

Table VIII. Effects of Polymer Thermal Expansion on SAW Sensor Frequencies

Polymer	158 MHz SAW Device		200 MHz SAW Device	
	kHz <sup>a</sup>	-Hz/°C <sup>b</sup>	kHz	-Hz/°C
Fluoropolyol	242	600	259	550
	254	600		
Poly(epichlorohydrin)	294	700	277	700
	263	600		
Poly(isobutylene)	264	950	260	950
	294	1000		
	269	1200		

<sup>a</sup> Frequency decrease on applying the polymer overlay.

<sup>b</sup> Slopes determined over the 20-30°C temperature range, subtracting the inherent temperature drift of the bare device.

Table IX. Parameters for Polymer Thermal Expansion Effects

Polymer	$\alpha \times 10^4$ °C <sup>-1</sup>	$A_{SAW} \times 10^3$ °C <sup>-1</sup>	$A_{SAW} / \alpha$
Fluoropolyol	5.4 <sup>a</sup>	2.4	4.4
Poly(epichlorohydrin)	5.6 <sup>b</sup>	2.5	4.5
Poly(isobutylene)	6 <sup>c</sup>	3.6	6

<sup>a</sup> Determined from the density data in reference 1.

<sup>b</sup> Assumed to be the same as that of isotactic Poly(epichlorohydrin) in reference 40.

<sup>c</sup> Reference 39.

Table X. Estimates for Polymer Swelling at the Test Vapor Concentrations.

Vapor	FPOL		PECH		PIB	
	C <sub>s</sub> <sup>a</sup> g/L	Swelling <sup>b</sup> %	C <sub>s</sub> g/L	Swelling %	C <sub>s</sub> g/L	Swelling %
isooctane	0.75	0.11	2.36	0.34	8.57	1.2
1,2-dichloroethane	5.67	0.45	35.8	2.9	7.65	0.61
toluene	9.26	1.1	22.7	2.6	12.2	1.4
nitromethane	11.6	1.0	12.8	1.1	0.58	0.05
butanone	161.	20.	21.7	2.7	3.37	0.42
2-propanol			2.59	0.33		
1-butanol	17.2	2.1	3.95	0.49	0.60	0.07

<sup>a</sup> Calculated from the vapor phase concentrations in Table III and the GLC partition coefficients in Table II, using values from determination B unless the value is only available from determination A..

<sup>b</sup> The fractional volume increase was calculated assuming the volume of the swollen polymer is approximately equal to the volume of the polymer before swelling. See text.

The volume expansion due to vapor sorption can be estimated if the partition coefficient is known. The product of the experimental vapor phase concentration and the partition coefficient gives the concentration of vapor in the sorbent phase (see eq 2). The volume contributed by this concentration of vapor in the polymer can then be approximated by the volume of an equivalent amount of this vapor in its liquid state, i.e. from the reciprocal of the liquid density,  $\rho_L$ . This method provides a reasonable first approximation as long as the amount of vapor sorbed is greater than that which can be accommodated by existing free volume or by microvoids that might be in the polymer film. In Table X we estimate the % increase in volume due to swelling for our test vapors in our test polymers using the vapor concentrations and liquid densities in Table III and  $K_{GLC}$  values from Table II. It is apparent that the volume increase of the sorbent phase can be significant. Increases on the order of 1 or 2% are common, and if a strongly sorbed vapor is present at sufficient concentrations, expansion as high as 20% could occur.

Now consider the response of a sensor coated with 250 kHz of fluoropolyol to a vapor such as 1,2-dichloroethane, which is estimated to swell the fluoropolyol by 0.45% when the vapor phase concentration is 65100 mg/m<sup>3</sup>. We calculate that the gravimetric response should be -0.55 kHz based on a log K value of 1.94, whereas the effect of increasing the volume by 0.45% could be as much as -5 kHz. Thus, the volumetric effect could be significantly larger than the gravimetric effect. Similar calculations using other vapors and polymers result in the same conclusion.

To simplify the consideration of these effects we can convert the above arguments to algebraic form and derive an equation relating SAW vapor responses to the sum of gravimetric and swelling effects. First we define a variable,  $A_{SAW}$  representing the kHz change in frequency due to a 1°C change in temperature per kHz of coating on the device surface. The units reduce to °C<sup>-1</sup>, the same units as a coefficient of thermal expansion. Since coefficients of thermal expansion are symbolized with an  $\alpha$ , we chose a capital alpha subscripted with SAW to represent this variable. We can then derive the following equation.

$$\Delta f_v = (\Delta f_s C_v K / \rho_S) + (\Delta f_s C_v K / \rho_L) (A_{SAW} / \alpha) \quad (6)$$

In this equation,  $\Delta f_v$  now represents the total frequency shift on vapor sorption due to both gravimetric and swelling effects. The first term is the gravimetric effect exactly as in eq 2. The density of the sorbent phase,  $\rho_S$ , is an approximation for the mass of the sorbent

phase divided by the volume of the stationary phase containing the sorbed vapor (1). When the swelling is only a few percent, this approximation should be reasonable. In the second term,  $C_v K$  gives the concentration of vapor in the sorbent phase, and  $C_v K / \rho_L$  gives the volume fraction increase of the polymer due to vapor sorption, i.e. the amount of swelling, assuming

$$V_v / V_s \approx V_v / (V_s + V_v) \quad (7)$$

where  $V_s$  and  $V_v$  are the volumes of the sorbent phase and the liquid vapor. (Values for percent swelling given in Table X were calculated making this assumption.) The variable  $\alpha$  in eq 6 is the coefficient of thermal expansion of the polymer. Then  $(C_v K) / (\rho_L \alpha)$  estimates the temperature change required to produce a volume change by thermal expansion that is equivalent to the estimated volume change caused by swelling. The product  $\Delta f_s A_{SAW}$  gives the frequency change that would be expected per degree of temperature change. Therefore, the second term as a whole gives the frequency change that might be expected if the estimated volume change due to swelling produces the same effect as an equivalent volume change due to thermal expansion.

Eq 6 predicts that sensor responses should be linearly proportional to partition coefficients, as we have observed (see Figure 3). Responses will also be proportional to the gas phase vapor concentration, as one would expect. Changes in the vapor concentration affect the gravimetric and swelling terms equally. The relative magnitudes of gravimetric and swelling effects depend primarily on the ratio of  $A_{SAW}$  to  $\alpha$ , and secondarily on the ratio of  $\rho_S$  to  $\rho_L$ . The ratio of  $A_{SAW} / \alpha$  is the more important factor because typical liquid and polymer densities are usually similar.  $A_{SAW}$  values calculated from our experimental SAW data are given in Table IX;  $A_{SAW} / \alpha$  ratios (also in Table IX) are between 4 and 6. Therefore, this model predicts that sorbent phase swelling effects will significantly exceed gravimetric effects.

Although we will evaluate this model quantitatively below, it was not our main intent to develop a quantitatively accurate model. Rather, we developed the model to rationalize why observed SAW sensor responses should exceed the gravimetric responses we determined from GLC partition coefficients and eq 2. The model is quite effective in this regard. The model and the rationale behind it show that it is virtually inevitable that sensor responses should exceed mass-loading effects considering the profound effect of polymer thermal expansion on sensor frequencies. The model shows that the differences between  $K_{GLC}$  values and  $K_{SAW}$  values (calculated according to eq 2) are not due to

systematic errors in our measurements. Rather, they reflect the true behavior of the sensors in response to vapor sorption by the polymer.

We can summarize the strengths of our model as follows: it is expressed in quantities that can be measured or reasonably estimated from measured quantities; it approximates for the first time the magnitude of the swelling effect; it shows that the swelling effect can greatly exceed the gravimetric effect; and it is in reasonable agreement with experimental observations. The model has a number of weaknesses residing in the assumptions made to estimate swelling effects. First, it is assumed that identical volume changes due to swelling (on vapor sorption) or thermal expansion will produce identical frequency changes. This may not be strictly correct since there are physical differences between the two cases: added small molecules are present in the polymer in the first case and not in the latter. Second, small changes in volume due to thermal expansion over a small interval are used to estimate potentially larger volume changes due to swelling. Third, the volume change due to swelling is estimated simply from the liquid density. Fourth, the model does not consider the effects of strong oriented interactions (such as hydrogen bonding) that may occur between the vapor and the polymer.

Our model (represented by eq 6) is evaluated quantitatively in Table XI using  $K_{GLC}$  values as the accurate partition coefficient values and presenting sensor responses in Hz. First the gravimetric responses predicted by eq 2 (or the first term in eq 6) are calculated. Then the observed responses of 200 MHz resonator vapor sensors are given, followed by the ratios of the observed responses to the gravimetric responses. These ratios are typically 4 to 6 as we have discussed previously in terms of  $K_{SAW}$  values. These results are in agreement with the generalization based on  $A_{SAW}/\alpha$  ratios that swelling effects should exceed gravimetric effects by 4 to 6 times. The differences between observed and gravimetric responses are reported as "excess" responses in the table. These numbers will be important when discussing modulus effects below. Then the responses predicted by our swelling model (eq 6) are reported. The actual responses of poly(isobutylene)-coated sensors and those predicted by eq 6 are in very reasonable agreement. The good agreement may reflect the fact that this polymer is non-polar and interacts with vapors primarily by "ideal" dispersion interactions. With poly(epichlorohydrin) the responses predicted by eq 6 are about twice the observed responses, suggesting that the model has overestimated swelling effects in this case, or that some third factor exists which opposes mass and swelling effects. With fluoropolyol, the most polar polymer of the group, the results are mixed. Agreement is reasonable for dichloroethane, but the responses predicted by eq 6 are about 2.3 times actual responses for three other vapors. The model predicts a spectacularly large result for butanone. In this particular case poor agreement is not

surprising given the extremely large swelling predicted for butanone. For most of the polymer/vapor pairs evaluated in Table XI, the model given by eq 6 agrees with our experimental results to within a factor of about 2. We believe that this is reasonable considering the approximations made to estimate swelling effects.

For predictive purposes, the model can be simplified in two ways. First, the ratio of  $A_{SAW}/\alpha$  in eq 6 could be replaced by an integer so that measurements of polymer thermal expansion and its effects on frequency would not be required to estimate sensor responses. This approach would retain the effects of polymer and vapor densities. The values in Table IX suggest that 4 would be an appropriate integer for general purposes. Although this works well for poly(isobutylene), we find empirically that a value of 2 would work better for poly(epichlorohydrin) and fluoropolyol. This approach is not altogether satisfying. Therefore we further simplify estimations by dropping considerations of vapor densities and suggesting that the swelling effect is 3 times the gravimetric effect. Then:

$$\Delta f_v = 4 \Delta f_s C_v K / \rho_s \quad (8)$$

This rule of thumb actually provides reasonable results for all three polymers. These predictions are listed in the last column of Table XI. Eq 8 predicts responses for ten of the 18 polymer/vapor pairs in Table XI to within +/-25%. All but three are predicted to within +/-35%. Eq 8 provides the simplest predictive model, while eq 6 provides the best conceptual model. The factor of 4 in eq 8 is justified by the conceptual model and by our experimental data.

Our comparisons of SAW and GLC results began in terms of partition coefficients, so we will conclude this section by comparing all the models in these terms. Partition coefficients are calculated from observed SAW sensor responses according to eq 2, 6, and 8 and reported as logs in Table XII. Values calculated according to eq 2 were previously denoted  $K_{SAW}$ , but we will now denote these with  $K_{SAW}^{eq 2}$  for clarity. Similarly, values calculated according to eq 6 and 8 are denoted  $K_{SAW}^{eq 6}$  and  $K_{SAW}^{eq 8}$ . The values calculated using the models that include swelling effects are significantly better than the model based on mass-loading effects alone.

Table XI. Comparisons of the Experimental Sensor Data with the Gravimetric and Swelling Models.

Poly(isobutylene)						
Vapor	Response: Gravimetric <sup>a</sup> eq 2 Hz	Response: Observed <sup>b</sup> Hz	Ratio: Observed/ Gravimetric	Response: Excess <sup>c</sup> Hz	Response: Swelling <sup>d</sup> eq 6 Hz	Response: Estimated <sup>e</sup> eq 8 Hz
isooctane	2610	17898	6.9	15290	23000	10000
1,2-dichloroethane	2330	10324	4.4	8000	13000	9300
toluene	3720	17774	4.8	14060	27000	15000
nitromethane	178	886	5.0	708	1000	710
butanone	1030	6304	6.1	5280	8100	4100
1-butanol	182	2158	12	1980	1400	730

Poly(epichlorohydrin)						
Vapor	Response: Gravimetric eq 2 Hz	Response: Observed Hz	Ratio: Observed/ Gravimetric	Response: Excess Hz	Response: Swelling eq 6 Hz	Response: Estimated eq 8 Hz
isooctane	440	1949	4.4	1510	4300	1800
1,2-dichloroethane	6680	19890	3.0	13210	39000	27000
toluene	4250	13671	3.2	9420	34000	17000
nitromethane	2380	9003	3.8	6620	15000	9500
butanone	4060	17747	4.4	13690	35000	16000
2-propanol	484	2896	6.0	2410	4200	1900
1-butanol	737	3293	4.5	2560	6200	2900

Table XI. Continued.

Vapor	Fluoropolyol					
	Response: Gravimetric eq 2 Hz	Response: Observed Hz	Ratio: Observed/ Gravimetric	Response: Excess Hz	Response: Swelling eq 6 Hz	Response: Estimated eq 8 Hz
1,2-dichloroethane	862	4747	5.5	3890	5900	3400
toluene	1410	5952	4.2	4540	13000	5600
nitromethane	1770	5736	3.2	3960	13000	7100
butanone	24500	37939	1.5	13400	248000	98000
1-butanol	2620	10958	4.2	8340	26000	10000

<sup>a</sup> Calculated according to eq 2 using  $K_{GLC}$  values as the accurate measure of partition coefficients.

<sup>b</sup> In all cases, the data from plasma-cleaned 200 MHz resonator sensors has been used.

<sup>c</sup> Observed response minus the gravimetric response.

<sup>d</sup> Responses calculated according to eq 6 including both gravimetric and swelling effects.

<sup>e</sup> Responses estimated using eq 8 as a simple approximate prediction.

Table XII. Comparisons of the Partition Coefficients Calculated from SAW Vapor Sensor Responses<sup>a</sup> by Various Models with Those Determined by GLC<sup>b</sup>.

Vapor	Poly(isobutylene)		
	log K <sub>GLC</sub>	log K <sub>SAW</sub> <sup>eq 2</sup>	log K <sub>SAW</sub> <sup>eq 6</sup>
isooctane	2.28	3.12	2.16
1,2-dichloroethane	2.07	2.72	1.99
toluene	2.76	3.44	2.57
nitromethane	1.55	2.25	1.48
butanone	1.80	2.59	1.69
1-butanol	2.20	3.27	2.38
			log K <sub>SAW</sub> <sup>eq 8</sup>
			2.51
			1.91
			2.84
			1.65
			1.99
			2.67
Vapor	Poly(epichlorohydrin)		
	log K <sub>GLC</sub>	log K <sub>SAW</sub> <sup>eq 2</sup>	log K <sub>SAW</sub> <sup>eq 6</sup>
isooctane	1.72	2.37	1.38
1,2-dichloroethane	2.74	3.21	2.41
toluene	3.03	3.54	2.59
nitromethane	2.89	3.47	2.62
butanone	2.61	3.25	2.28
2-propanol	2.17	2.95	1.96
1-butanol	3.02	3.67	2.70
			log K <sub>SAW</sub> <sup>eq 8</sup>
			1.76
			2.61
			2.94
			2.86
			2.65
			2.34
			3.07
Vapor	Fluoropolyol		
	log K <sub>GLC</sub>	log K <sub>SAW</sub> <sup>eq 2</sup>	log K <sub>SAW</sub> <sup>eq 6</sup>
1,2-dichloroethane	1.94	2.68	1.85
toluene	2.64	3.27	2.29
nitromethane	2.85	3.36	2.48
butanone	3.48	3.67	2.66
1-butanol	3.66	4.28	3.28
			log K <sub>SAW</sub> <sup>eq 8</sup>
			2.08
			2.66
			2.76
			3.07
			3.68

<sup>a</sup> Partition coefficients back-calculated from observed sensor responses using the data from plasma-cleaned 200 MHz resonator sensors.

<sup>b</sup> Using K<sub>GLC</sub> values taken from determinations B wherever possible.

**Modulus Effects.** The probable mechanism by which polymer swelling influences sensor frequencies is via the sensitivity of the SAW device to reductions in the modulus of the polymer overlayer. Until now the relative magnitudes of mass and modulus effects during vapor sorption have not been known, nor was it possible to estimate modulus effects from theoretical models. Now that it has been demonstrated that mass effects are only a fraction of the total sensor response, and we have numerical calculations for the extent to which responses exceed gravimetric responses (the "excess" response), it is worthwhile to re-examine the role of modulus effects. We begin our treatment with an equation derived by Wohltjen to describe the effect of a thin non-conducting overlay film of thickness  $h$  and density  $\rho$  applied to the SAW device surface (3).

$$\Delta f_s = (k_1 + k_2) F^2 h \rho - k_2 F^2 h (4 \mu / V_R^2) [ (\lambda + \mu) / (\lambda + 2\mu) ] \quad (9)$$

In this equation,  $F$  is the fundamental resonant frequency of the oscillator, and  $\Delta f_s$  is the change in frequency caused by the film. The constants  $k_1$  and  $k_2$  are material constants for the piezoelectric substrate, and  $V_R$  is the Rayleigh wave velocity in that substrate. The parameters  $\lambda$  and  $\mu$  describe the physical properties of the overlay film material, being the Lamé' constant and the shear modulus, respectively. The film mass per unit area,  $m/A$ , is customarily substituted for  $h/\rho$ ; both quantities have the same units. Then the first term represents the gravimetric effects, and the second represents the modulus effects.

In order to illustrate the role of modulus changes in sensor responses with some calculations, we will consider a 200 MHz quartz SAW device coated with a polymer to a thickness of 50 nm. The density of the polymer material is assumed to be 1 g/mL. The Rayleigh wave velocity in quartz is taken as 3300 m/sec and values of  $-9 \times 10^{-8}$  and  $-4 \times 10^{-8} \text{ m}^2 \text{ sec kg}^{-1}$  are used for  $k_1$  and  $k_2$  (1,3). The frequency shift due to the mass of the coating calculated from the first term in eq 9 is then -260 kHz. Thus, this example is similar to the SAW sensors we have actually investigated.

The contribution of the second term in eq 9 depends on the modulus of the polymer film on the surface as it is perceived by the high frequency surface waves. If the modulus of the polymer film is  $1 \times 10^9 \text{ N/m}^2$ , a value typical of glassy polymers, then the second term in eq 8 contributes +29 kHz to  $\Delta f_s$ . If the modulus is only  $1 \times 10^6 \text{ N/m}^2$ , a value typical of a rubbery polymer, then the second term in eq 9 is negligible relative to the first

term. (In these and all other calculations of modulus effects we make the simplifying assumption that the quantity  $(\lambda + \mu) / (\lambda + 2\mu)$  is always ca. 1. This term is algebraically constrained to values between 0.5 and 1.0. Since  $\lambda$  is typically greater than  $\mu$ , it is further constrained to values between 0.67 and 1.)

Although we typically choose soft rubbery polymers for our sensor coatings, it is not correct to assume that  $1 \times 10^6 \text{ N/m}^2$  is the correct modulus value to use in calculations. The measurement of modulus in viscoelastic polymers is highly frequency dependent (41,42). At the frequencies of our SAW devices the surface waves will sense the film as a stiff glassy material rather than as a soft rubbery material. This effect occurs because the acoustic waves couple into the film, inducing strains at high frequencies (43,13). If the characteristic relaxation time of the polymer is longer than the period of these strains, the polymer will appear to be stiff to the probing waves. As a result, the magnitude of the second term of eq 9 when a rubbery material is applied to the SAW surface will likely approach that which is calculated using a modulus value of ca.  $10^9 \text{ N/m}^2$ .

(Nevertheless, we emphasize that the state of the polymer material is unchanged. If the film were simultaneously probed by a slow measurement technique, one would obtain the modulus characteristic of the slower measurement, i.e. that of a rubber. This argument follows from the Boltzman superposition principle (41,42).)

Eq 9 and our subsequent calculations address the effect of applying the polymer film to the device surface. To derive the effect of vapor sorption it is useful to rewrite eq 9 for the application of a polymer film which contains the sorbed vapor.

$$\Delta f_s' = (k_1 + k_2) F^2 m' / A - k_2 F^2 h (4 \mu' / V_R^2) [ (\lambda' + \mu') / (\lambda' + 2\mu') ] \quad (10)$$

The primes in eq 10 denote the properties of the film with the vapor. The difference between the effects of the film with and without the sorbed vapor give the effect of the vapor. This difference is obtained by subtracting eq 9 from 10. The two terms for gravimetric effects reduce to

$$\Delta f_v (\text{gravimetric}) = (k_1 + k_2) F^2 m_v / A \quad (11)$$

Thus,  $\Delta f_v$  in this case is the gravimetric response due to the mass of sorbed vapor,  $m_v$ . This well-known equation was the basis for the derivation of eq 2. The advantage of eq 2 is that the partition coefficient can be evaluated independently, whereas the value of  $m_v / A$  in eq 11 is not known directly.

The terms for the film modulus effects reduce to

$$\Delta f_v (\text{modulus}) = k_2 F^2 h (4 \mu / V_R^2) [ (\lambda + \mu) / (\lambda + 2\mu) ] - k_2 F^2 h (4 \mu' / V_R^2) [ (\lambda' + \mu') / (\lambda' + 2\mu') ] \quad (12)$$

In order to evaluate these modulus effects, it is necessary to know the initial modulus of the film (without vapor) and the final modulus of the film containing the vapor. Neither of these is actually known, and this is the reason that the effects of modulus changes have been difficult to evaluate in the past. Nevertheless, we can now make some estimates and compare them with our experimental excess responses.

Eq 12 shows that the initial modulus of the film in the first term is very important in determining the potential for polymer softening to influence vapor sensor responses. If the film softens to the point where the second term in eq 12 is negligible relative to the first, then the maximum possible decrease in frequency due to polymer softening is the value of the first term. As we calculated above, this value will be -29000 Hz when the initial modulus of the polymer film (as it is perceived by the high frequency surface waves) is  $1 \times 10^9 \text{ N/m}^2$ . The fact that this number is large relative to a typical sensor response demonstrates that modulus effects could contribute significantly to sensor responses. However, if the initial polymer modulus is only  $1 \times 10^8 \text{ N/m}^2$ , then the maximum decrease in frequency due to softening is only 2900 Hz. The softer the initial modulus, the less that modulus effects can contribute to the vapor sensor response.

We can use our experimental results to set lower limits for the initial moduli of our polymer films as follows. First, we note that our calculations above show that sensor frequencies decrease by ca. 2900 Hz for each  $1 \times 10^8 \text{ N/m}^2$  decrease in modulus. Second we assume that the excess sensor responses observed are entirely due to changes in polymer modulus. The excess responses (see Table XI) are ca. 8000 to 15000 Hz for vapors causing greater than 10000 Hz of response. This suggests that polymer moduli are softening by 3 to  $5 \times 10^8 \text{ N/m}^2$  upon vapor sorption. The largest excess response on the poly(isobutylene)-coated sensor is 15000 Hz (isooctane), indicating a modulus change of ca.  $5 \times 10^8 \text{ N/m}^2$ . Therefore, the initial modulus of the film cannot be less than ca.  $5 \times 10^8 \text{ N/m}^2$ . Similar analysis of the data for the other two coating materials suggest limiting moduli of ca.  $4 \times 10^8 \text{ N/m}^2$  for poly(epichlorohydrin) and fluoropolyol. These numbers are entirely reasonable compared to a typical value of  $10^9 \text{ N/m}^2$  for a glassy polymer.

The lower limit to the modulus of fluoropolyol was calculated based on the response to butanone. These data are particularly interesting. The observed response of 37000 Hz is the largest response reported. All others were less than 20000 Hz. The

excess response in this case is only 13000 Hz, which is only half the gravimetric response. All other vapor/polymer pairs produced excess responses of at least twice the gravimetric response, and ratios of three to five were most common. The implications of these results are that the amount of butanone sorbed has exceeded the amount required to fully soften the polymer, i.e. to soften it to the point where further softening does not produce any further frequency response on the sensor. In this case, the lower limit for the initial modulus calculated above for fluoropolyol is likely to be the actual initial modulus.

These discussions ultimately lead to the question of precisely how the film modulus of the polymer changes with the concentration of vapor in the film. Over small increments near the initial modulus of the film, the relationship might be linear. Alternatively, over large ranges, one might ask: 'Does doubling the amount of vapor that causes one decade of modulus decrease cause the modulus to decrease by a second decade?'. The answers to these questions simply are not known yet. However, now that we have shown that these sensors are not simple gravimetric sensors, the questions become rather important. We can only predict, based on eq 12 and the discussion above, that once a vapor concentration has been reached that decreases the modulus by one decade, further increases in vapor concentration will produce diminishing additional sensor responses due to modulus effects.

*Note that this means that the vapor sensor response relative to the concentration of vapor in the film will become non-linear at high concentrations. Then the sensor calibration curve, i.e., the vapor sensor response as a function of the gas phase vapor concentration, would be non-linear even if the sorption isotherm were linear. Therefore, polymer-coated SAW vapor sensor calibration curves cannot necessarily be equated with sorption isotherms. Such an equivalence will only be valid when the mass and modulus responses are both linear with gas phase vapor concentration over the full concentration range of the isotherm.*

It is useful to compare the effects of modulus as discussed above with our swelling model. As we have noted previously, the likely effect of swelling is to reduce the modulus. Then the second term in eq 6 is a greatly simplified approximation for the modulus effect in eq 12. The advantage of the swelling term in eq 6 is that it is expressed in quantities that allow predictions to be made. The models are similar in predicting that these effects should be proportional to film thickness.

However, the swelling and modulus models differ significantly in how they predict the effects of vapor sorption over large concentration ranges. Eq 6 simply predicts that the swelling effect will be linear with vapor concentration. Eq 12 and the discussion above showed that there are finite limits to modulus effects. Therefore the second term in eq 6 will overestimate swelling effects once sufficient vapor has been sorbed to render further

modulus changes insignificant. Indeed, eq 6 spectacularly overestimated the response of the fluoropolyol-coated sensor to butanone.

Recently Bartley and Dominguez have proposed a model for polymer-coated SAW sensor responses that contains three terms (12). Mass-loading effects are predicted to decrease sensor frequencies as usual. A term for modulus effects predicts that polymer softening should decrease frequencies in accord with previous models and our results in this paper. These authors include a third term for elastic effects associated with a hypothetical compressive tension. This term opposes mass loading and polymer softening effects. It is suggested that this "tightening" might occur on polymer thermal expansion or swelling during vapor sorption. No experimental evidence was provided to demonstrate the existence of this hypothetical effect, nor is it clear if such tightening could occur in a soft rubbery polymer which is capable of polymer chain motion in response to vapor sorption or thermal expansion. We can conclude from our results that this tightening term cannot be dominant in either vapor sorption or thermal expansion experiments. We demonstrated above that thermal expansion causes SAW frequencies to decrease, not increase, and vapor sorption causes SAW frequencies to decrease by an amount which is up to ca. 4 times the gravimetric effect. In terms of Bartley's model, one must conclude that the modulus terms predominate in each case.

We must emphasize that Bartley and Dominguez use the word swelling specifically in reference to their compressive tension term. Our use of the word swelling includes all effects not accounted for by mass loading, including polymer softening on vapor sorption. There is no conflict between our conclusion that swelling decreases SAW frequencies and Bartley's proposal that swelling, as it specifically refers to the proposed tightening, increases SAW frequencies.

It is interesting to note a few more aspects of this model. All effects are predicted to be proportional to film thickness. This lends further support to our assumption in the definition of our  $A_{SAW}$  term that thermal expansion effects should be proportional to the amount of polymer on the device surface. In addition, we have noted that responses predicted by our two term model (eq 6) often exceeded actual sensor responses. This is consistent with the possible existence of a third term which opposes mass-loading and softening, such as Bartley's tightening term. However, any conclusion about the existence or magnitude of such tightening effects on this basis would be tenuous.

A viscoelastic model for SAW sensor behavior has recently been reported by Martin and Frye (13). They considered polymer relaxation behavior as it is influenced by raising the polymer temperature or by plasticization occurring in response to the sorption of vapors. Their model should be useful whenever the sensor operating temperature is at or

somewhat below the temperature of a polymer relaxation process at the sensor operating frequency, and the relaxation process influences sensor frequency. Under these circumstances, the polymer will be plasticized by sorbed vapor, inducing the relaxation process to occur at the sensor temperature and altering the sensor frequency. For the specific case these authors examined, a styrene-butadiene-styrene triblock copolymer, the relaxation process observed caused the sensor frequency to increase such that relaxation effects opposed the mass-loading response during vapor exposures. The modulus of this triblock copolymer was unchanged through the relaxation process, whereas the viscosity decreased. These studies demonstrated that viscosity decreases cause the sensor frequency to increase.

This model, at least as it applies to the specific case examined, cannot be extended to our results. Our frequency responses were enhanced relative to gravimetric effects, whereas those of the triblock copolymer were decreased relative to gravimetric effects. In addition, homogeneous amorphous polymers of the types we investigate undergo large changes in both modulus and viscosity during the primary relaxation processes involving polymer chain segments. It is therefore not clear if the results obtained with the triblock copolymer, i.e., that the modulus is relatively constant and the relaxation process causes frequencies to increase, can be generalized to our polymers. However, it is useful to consider viscosity effects. If viscosity decreases are occurring on vapor sorption and they exceed the viscosity decreases during polymer thermal expansion (for an equivalent volume change), then this could account for why our swelling model based on thermal expansion overestimates actual SAW sensor responses. This hypothesis seems plausible considering that vapor sorption adds small molecules to the film, and polymer thermal expansion does not. It is possible that viscous effects should be included in a model for SAW sensor response as a third factor that opposes mass and modulus effects.

**Comparisons with other Acoustic Devices.** The model represented by eq 6 is not limited to SAW devices. The first term for gravimetric effects is easily derived for other acoustic mass balances such as quartz crystal microbalance (QCM) and flexural plate wave (FPW) devices. The second term for swelling effects is also general and can be applied to these devices. Therefore, the relative roles of mass-loading and swelling effects in the responses of polymer-coated acoustic vapor sensors can be evaluated simply measuring the effects of polymer thermal expansion on device frequencies.

A number of these types of experiments have been conducted on FPW devices and the rates of frequency change with temperature are similar to those reported above using SAW devices (17, 44). These results imply that swelling (or modulus) effects are equally important on these two types of sensors. Furthermore, it has been shown that SAW and

FPW devices coated with poly(vinyl tetradecanal) to the same thicknesses in terms of kHz give similar responses to vapors (17, 44). The equivalence of SAW and FPW sensor responses has also been observed with fluoropolyol-coated sensors (45). This indicates that these two types of acoustic sensors are detecting vapors by the same mechanism, in which case our arguments above for the predominant role of swelling and modulus effects must apply.

Similar comparisons of polymer-coated SAW and QCM devices are not available. However, initial experiments in our laboratory indicate that QCM frequencies are also influenced by polymer thermal expansion. It may be worthwhile to re-examine the long standing assumption that vapor sensors based on polymer-coated QCM devices are gravimetric.

**Final Remarks.** We can summarize our arguments for the importance of polymer phase swelling in determining SAW vapor sensor responses as follows:

1. SAW vapor sensor responses exceed those expected based on mass effects alone, taking gas-liquid chromatography as an independent experimental measure of the mass-loading. We find this to be true regardless of the polymer or the SAW device used and despite extensive efforts on our part to eliminate any possible sources of systematic error in our measurements. In general SAW responses exceed gravimetric responses by 4 to 6 times. This relationship is clearest for polymers which are not capable of strong specific interactions with most vapors.

2. Thermal expansion provides a method to experimentally measure the effects of volume expansion on SAW frequencies which is independent of changes in mass per unit area. Volume changes associated with polymer thermal expansion have very significant effects on SAW frequencies. Frequencies change at rates of  $-0.6 \text{ kHz}/^\circ\text{C}$  or more on our polymer-coated sensors at around room temperature. Therefore, it is straightforward to expect that volume changes associated with vapor sorption will significantly influence sensor frequencies.

3. By analogy, acoustic velocities through bulk polymers are known to be affected by volume changes associated with polymer thermal expansion, so volume change effects on surface wave velocities are not surprising.

4. The swelling that occurs on vapor sorption can be estimated from partition coefficients and vapor liquid densities; volume increases of a few percent are typical. These volume increases are significantly higher than the amount of volume change that occurs on thermal expansion over small temperature ranges (typically 0.05% per degree).

5. We have derived a model which indicates that swelling effects should be in the range of 4 to 6 times gravimetric effects when polymer and vapor liquid densities are similar. Our experimental SAW vapor sensor responses were, indeed, typically 4 to 6 times those predicted by mass loading effects.

Our identification of swelling effects as a major contribution to SAW vapor sensor responses represents a profound change in thinking about how polymer-coated SAW sensors behave. Sensor responses are actually multiplied beyond the effect of vapor mass alone. The use of the term gravimetric in reference to such sensors is therefore misleading, since it is now apparent that such sensors are more sensitive to the changes in polymer viscoelastic properties that occur on vapor sorption. The effect of the vapor's mass is actually minor in comparison.

With this fundamental revision in understanding, it may be possible to exploit this aspect of sensor response to gain more sensitive or selective sensors. Thus, it might be worthwhile to select polymers with large dynamic moduli under the SAW operating conditions in order to obtain the greatest potential for modulus effects. In this case, one would choose a polymer above its  $T_g$  at the sensor operating temperature to facilitate vapor diffusion, but well below the temperatures of relaxation processes that reduce the dynamic modulus. The swelling model further indicates that if the same mass of vapor is sorbed at the surfaces of two sensors, one of which sorbs it by adsorption on the surfaces of a hard porous coating, while the other absorbs it into a sorbent polymer phase, the latter will give a significantly larger response.

## ACKNOWLEDGEMENT

The authors would like to acknowledge Dr. Stephen Martin stimulating discussions on viscoelastic models for SAW sensor response, Dr. Lloyd Burgess for discussions of refractive index and thickness changes in polymers on vapor sorption, and Dr. Richard M. White for discussions on ultrasonic sensors and the effects of density and modulus on acoustic velocities.

This work was supported by funds from the Office of Naval Technology administered by the Naval Surface Warfare Center, Dahlgren, VA, and by funds from the the Office of Naval Research administered by the Naval Research Laboratory.

## REFERENCES

1. Grate, J.W.; Snow, A.; Ballantine, D.S., Jr.; Wohltjen, H.; Abraham, M.H.; McGill, R.A.; Sasson, P. *Anal. Chem.* 1988, 60, 869-875.
2. Ballantine, D.S., Jr.; Rose, S.L.; Grate, J.W.; Wohltjen, H. *Anal. Chem.* 1986, 58, 3058-3066.
3. Wohltjen, H. *Sens. Actuators* 1984, 5, 307-325.
4. Snow, A.; Wohltjen, H. *Anal. Chem.* 1984, 56, 1411-1416.
5. Ballantine, D.S., Jr.; Wohltjen, H. *Anal. Chem.* 1989, 61, 704A-715A.
6. Fox, C.G.; Alder, J.F. *Analyst* 1989, 114, 997-1004.
7. D'Amico, A.; Verona, E. *Sens. Actuators* 1989, 17, 55-66.
8. Nieuwenhuizen, M.S.; Venema, A. *Sensors and Materials* 1989, 5, 261-300.
9. Bastiaans, G.J. *Chemical Sensors*, Edmonds, T.E. Ed.; Blackie: Glasgow and London, 1988, 295-319.
10. Grate, J.W.; Abraham, M.H. *Sens. Actuators* 1991, in the press.
11. McCallum, J.J. *Analyst(London)* 1989, 114, 1173-1189.
12. Bartley, D.L.; Dominguez, D.D. *Anal. Chem.* 1990, 62, 1649-1656.
13. Martin, S.J.; Frye, G.C. *Appl. Phys. Lett.* 1990, 57, 1867-1869.
14. Janghorbani, M.; Freund, H. *Anal. Chem.* 1973, 45, 325-332.

15. Edmunds, T.E.; West, T.S. *Anal. Chim. Acta* 1980, 117, 147-157.
16. McCallum, J.J.; Fielden, P.R.; Volkan, M.; Alder, J.F. *Anal. Chim. Acta* 1984, 162, 75-83.
17. Grate, J.W.; Wenzel, S.W.; White, R.M., *Anal. Chem.* 1991, in the press.
18. Grate, J.W.; Klusty, M. NRL Memorandum Report 6762, 1990.
19. Grate, J.W.; Ballantine, D.S., Jr.; Wohltjen, H. *Sens. Actuators* 1987, 11, 173-188.
20. Rose-Pehrsson, S.L.; Grate, J.W.; Ballantine, D.S., Jr.; Jurs, P.C. *Anal. Chem.* 1988, 60, 2801-2811.
21. Grate, J.W.; Klusty, M.; Barger, W. R.; Snow, A.W. *Anal. Chem.* 1990, 62, 1927-1934.
22. Field, D.E. *J. Paint Technol.* 1976, 48, 43.
23. Abraham, M.H.; Grellier, P.L.; McGill, R.A. *J. Chem. Soc., Perkin Trans. 1* 1987, 797-803.
24. Rezgui, N.; Alder, J.F. *Analytical Proceedings* 1989, 26, 46-48.
25. Bowers, W.D.; Chuan, R.L. *Rev. Sci. Instrum.* 1989, 60, 1297-1302.
26. Grate, J.W.; Klusty, M. , *Anal. Chem.* 1991, in the press.
27. Bowers, W.D.; Duong, R.; Chuan, R.L. *Rev. Sci. Instrum.* 1991, in the press.
28. *Handbook of Chemistry and Physics, 51st Edition*; Weast, R.C., Ed.; The Chemical Rubber Co.: Cleveland, 1970.

29. Conder, J.R.; Young, C.L. *Physicochemical Measurement by Gas Chromatography*; John Wiley & Sons: New York, 1979.
30. Rogers, C.E. in *Polymer Permeability*; Comyn, J., Ed.; Elsevier: New York, 1985; pp. 11-73.
31. Roe, R.-J. in *Encyclopedia of Polymer Science and Engineering*, Vol 7, 2nd Ed., John Wiley and Sons, Inc.: New York, 1987; pp 531-544.
32. Massines, R.; Piche, L.; Lacabanne, C. *Makromol. Chem., Macromol. Symp.* 1989, 23, 121-137.
33. Hartman, B. in *Encyclopedia of Polymer Science and Engineering*, Vol 1, 2nd Ed., John Wiley and Sons, Inc.: New York, 1984; pp 131-160.
34. Work, R. *J. Appl. Phys.* 1956, 27, 69-72.
35. Wada, Y.; Yamamoto, K. *J. Phys. Soc. Jpn.* 1956, 11, 887-892.
36. Kwan, S.F.; Chen, F.C.; Choy, C.L. *Polymer* 1975, 16, 481-488.
37. Ballantine, D. S., Jr.; Wohltjen, H. in *Chemical Sensors and Microinstrumentation*, ACS Symposium Series 403, American Chemical Society: Washington, D.C., 1989; pp 222-236.
38. Wrasidlo, W. in *Advances in Polymer Science*, Vol. 13, Springer-Verlag: New York, 1974; pp 29-53.
39. Lewis, O.G. in *Physical Constants of Homopolymers*, Springer Verlag: New York, 1968; p 25.
40. Adamson, A.W. *A Textbook of Physical Chemistry*, Academic Press: New York, 1973; p. 319.

41. Aklonis, J.J.; MacKnight, W.J.; Shen, M. *Introduction to Polymer Viscoelasticity*, Wiley-Interscience: New York, 1972
42. Ferry, J.D. *Viscoelastic Properties of Polymers*, 3rd. Ed. John Wiley and Sons, Inc.: New York, 1980.
43. Wohltjen, H.; Dessy, R.E. *Anal. Chem.* 1979, *51*, 1458-1475.
44. Grate, J.W.; Wenzel, S.W.; White, R.M., NRL Memorandum Report 6815, April, 1991.
45. Grate, J.W.; Wenzel, S.W.; White, R.M., unpublished results.